Quantitative Economics 11 (2020), 1485–1520 1759-7331/20201485

Inflation and professional forecast dynamics: An evaluation of stickiness, persistence, and volatility

Elmar Mertens
Research Centre, Deutsche Bundesbank

James M. Nason
Department of Economics, NC State University and Centre for Applied Macroeconomic Analysis

This paper studies the joint dynamics of U.S. inflation and a term structure of average inflation predictions taken from the Survey of Professional Forecasters (SPF). We estimate these joint dynamics by combining an unobserved components (UC) model of inflation and a sticky-information forecast mechanism. The UC model decomposes inflation into trend and gap components, and innovations to trend and gap inflation are affected by stochastic volatility. A novelty of our model is to allow for time-variation in inflation-gap persistence as well as in the frequency of forecast updating under sticky information. The model is estimated with sequential Monte Carlo methods that include a particle learning filter and a Rao–Blackwellized particle smoother. Based on data from 1968$Q4$ to 2018$Q3$, estimates show that (i) longer horizon average SPF inflation predictions inform estimates of trend inflation; (ii) inflation gap persistence is countercyclical before the Volcker disinflation and acyclical afterwards; (iii) by 1990 sticky-information inflation forecast updating is less frequent than it was earlier in the sample; and (iv) the drop in the frequency of the sticky-information forecast updating occurs at the same time persistent shocks become less important for explaining movements in inflation. Our findings support the view that stickiness in survey forecasts is not invariant to the inflation process.

Keywords. Inflation, sticky information, professional forecasts, unobserved components, stochastic volatility, time-varying parameters, Bayesian, particle filter.

JEL classification. C11, C32, E31.

Elmar Mertens: elmar.mertens@bundesbank.de
James M. Nason: jmnason@ncsu.edu

We thank Gregor Smith for several conversations that motivated this paper. We also received valuable comments from three anonymous referees, Todd Clark, Patrick Conway, Drew Creal, Bill Dupor, Andrew Filardo, Monica Jain, Alejandro Justiniano, and Wolfgang Lemke and suggestions from colleagues and participants at numerous seminars and conferences. Jim Nason thanks the Jenkins Family Economics Fund at North Carolina State University for financial support. The views herein are those of the authors and do not represent the views of the Deutsche Bundesbank or the Eurosystem. Replication material and additional results are available at https://github.com/elmarmertens/MertensNasonQEstickyinformation.

1. Introduction

Central banks pay particular attention to inflation expectations. For example, Bernanke (2007) argued that well-anchored inflation expectations are necessary for a central bank to stabilize inflation. A reason for the concern is that inflation expectations express private agents' beliefs about the underlying factors driving observed inflation dynamics. A problem is central bank policy makers lack direct knowledge of these latent factors. Instead, they have to infer the causes of inflation dynamics from other sources.

Surveys of professional forecasts are valuable sources of information about the path of future inflation. Among others, Faust and Wright (2013) and Ang, Bekaert, and Wei (2007) recognized surveys of professional forecasts yield predictions of inflation that often dominate model-based out of sample forecasts. The inflation forecasting literature also documents that there is time-variation in the long-run mean of inflation around which "good" forecasts should be centered; see, for example, Stock and Watson (2007) and Faust and Wright (2013). In particular, Faust and Wright stressed the value of survey expectations in tracking low-frequency variation in inflation, also known as movements in "trend inflation." In contrast, measures of real activity (i.e., output and unemployment rate gaps) have been found to give only weak signals for inflation forecasting over above and beyond the information contained in survey forecasts.[1]

Notwithstanding the merits of surveys of professional forecasts to predict inflation, these forecasts are known to be biased and inefficient. Coibion and Gorodnichenko (2012, 2015) showed predictable survey forecast errors to be consistent with the sticky-information framework of Mankiw and Reis (2002) and models of noisy information or rational inattention as in Woodford (2003), Sims (2003) and Mackowiak and Wiederholt (2009). Conveniently, sticky and noisy information models yield a partial adjustment equation that relates the current survey forecast to a weighted average of the previous period's survey forecast and the current rational-expectations forecast.[2] We call this partial adjustment equation the "sticky-information law of motion of inflation forecasts" and its partial adjustment coefficient, which reflects the sluggishness of survey forecasts in updating toward rational expectations, the "sticky-information weight."[3]

Our paper studies the joint dynamics of realized inflation and inflation predictions collected from the Survey of Professional Forecasters (SPF). The SPF offers a particular long time series of survey responses, which allows us to document time variation in survey stickiness in connection with long-running changes in the inflation process. We model the average survey response as a sticky-information (SI) forecast to account for predictable forecast errors in the SPF. We combine the SI law of motion for survey forecasts with a time-series model that generates rational-expectations (RE) forecasts of inflation as inputs for the SI updating equation. Among the voluminous literature that

[1] Stock and Watson (1999, 2009) found a diminished role for activity-based forecasts of inflation, at least, since the mid 1980s. Their results are confirmed by, among others, Atkeson and Ohanian (2001), Hansen, Lunde, and Nason (2011), and Faust and Wright (2013).

[2] Coibion and Gorodnichenko (2012, 2015) derived the partial adjustment equation by aggregating individual survey responses across participants, and the resulting law of motion pertains to the cross-sectional average of survey responses.

[3] We do not further distinguish between the underlying sticky- or noisy-information models.

studies the dynamics of inflation and survey forecasts, our paper is closest to Kozicki and Tinsley (2012), and Henzel (2013)—who model survey forecasts as RE—as well as Mertens (2016), and Nason and Smith (forthcoming)—who allow surveys to differ from RE forecasts.

A particular innovation of our paper is stochastic drift in the sticky-information weight. Drift in stickiness captures changes in the sensitivity of survey forecasts to incoming data, which could arise, for example, due to time-varying attention levels. We use our model to ask whether the sticky-information weight has been changing over time, and whether this change appears related to changes in the inflation process, notably its persistence. Indeed, we find important changes in forecast stickiness that coincide with changes in inflation persistence over the post-war sample.[4] Persistence means that inflation is predictable, and we find that stickiness has risen when the resulting inefficiency in SI forecasts has been relatively small. These results are consistent with the evidence of Croushore (2010) who reports that the predictability of survey errors tends to be episodic and hard to exploit in real time.

The SI law of motion of inflation forecasts takes RE inflation forecasts as inputs. While we can abstract from the fundamental determinants of inflation, a good mechanism for generating RE forecasts is required. We use a version of the Stock and Watson (2007) unobserved components (UC) model of inflation as the source of RE forecasts. Canonical features of the Stock–Watson (SW-)UC model are a decomposition into trend and gap components, random-walk dynamics of the trend, and stochastic volatility in innovations to trend and gap inflation. Stock and Watson (2007) documented important time-variation in inflation in U.S. post-war data. In their UC model, time-varying persistence is captured via changes in the relative importance of the stochastic volatilities attributed to trend and gap shocks. In subsequent work, Cogley, Primiceri, and Sargent (2010) highlighted further time-variation in gap persistence, while Stock and Watson (2016) found that highly transitory shocks account for a large share of quarterly changes in inflation since 2000.

We build on these results with a UC representation of inflation as the sum of a trend and two gap components. The inflation gap is modeled as the sum of a persistent cyclical component and an irregular component that captures highly transitory shocks to inflation as well as measurement error. The cyclical component is modeled as an AR(1), and its autoregressive coefficient is labeled the "inflation gap persistence parameter." Goodfriend and King (2005) and Meltzer (2014) contended that movements in inflation at the business cycle frequencies changed after the 1980s. We estimate models with static and drifting inflation gap persistence to evaluate their claims.

The combination of our SW-UC model, the SI law of motion of inflation forecasts, and the term structure of average SPF inflation predictions yields a nonlinear state space model. We consider four different specifications of the model; all feature stochastic volatility in trend and gap inflation, but the models differ in whether there is drift

[4]Stickiness characterizes the extent to which SI forecasts represent smoothed RE forecasts. In contrast, inflation persistence characterizes serial correlation in inflation. By one measure, persistence is the time needed for inflation to revert to trend (or steady state) in response to a shock.

in the sticky-information weight, the gap persistence coefficient, or both. The latent factors of the inflation process are well identified by conditioning our estimates on the term structure of SPF predictions in addition to inflation data.

An important contribution is our strategy for estimating the four nonlinear state space models. We employ the particle learning filter proposed by Carvalho, Johannes, Lopes, and Polson (2010) and a Rao–Blackwellized particle smoother developed by Lindsten, Bunch, Särkkä, Schön, and Godsill (2016) for this task.[5] Particle learning allows us to update parameter estimates over the course of the sample. Inflation forecasts generated by particle learning mimic the real-time environment of the SPF. The particle learning filter and Rao–Blackwellized particle smoother are state of the art sequential Monte Carlo (SMC) methods that are new to empirical macroeconomics.[6]

The state space models are estimated on GNP/GDP deflator inflation and the average SPF nowcast and 1-, 2-, 3-, and 4-quarter ahead inflation predictions. The sample runs from 1969Q1 to 2018Q3.[7]

We report strong evidence in favor of the state space model in which the inflation gap persistence parameter and sticky-information weight drift. Estimates of this state space model show (i) the 4-quarter ahead average SPF inflation prediction improves the efficiency of estimates of trend inflation, (ii) comovement in the inflation gap persistence parameter and the business cycle shifts from countercyclical before the Volcker disinflation to no comovement after 1984, (iii) the frequency of sticky-information inflation forecast updating falls from less than two quarters on average pre-1990 to about 3 to 5 quarters on average post-1990, except during the 2007–2009 recession, and (iv) this change in the sticky-information weight lines up with a fall in the share of the variation of inflation explained by persistent shocks to trend and gap inflation.

Our results are useful for monetary policy makers and researchers. Estimates of our the state space model favored by the data display an inverse relationship between the frequency of sticky-information inflation forecast updating and the importance of persistent shocks to explain fluctuations in inflation. Our findings support the view that stickiness in survey forecasts is not invariant to the inflation process, and by extension, also not to the underlying monetary policy strategy. In particular, our results suggest that anchored expectations of inflation are coincident with infrequent updating of sticky-information forecasts of inflation. Leeper and Zha (2003) cautioned policy makers to avoid actions that cause persistent shifts in private-sector expectations. In a similar vein, our results suggest that central banks should guard against policies that lead the public to anticipate persistent variations in inflation.

[5]Our state space models can be Rao–Blackwellized because a subset of states are linear and Gaussian, given the nonlinear states. A good introduction to Rao–Blackwellization of particle filters is Creal (2012). Lopes and Tsay (2011) discussed the role of Rao–Blackwellization in particle learning filters.

[6]A recent example is Ascari, Bonomolo, and Lopes (2019). They estimate a small new Keynesian model with a particle learning filter, but do not utilize a particle smoother.

[7]Our goal is to study the impact of changing inflation dynamics on the beliefs of sticky-information forecasters at the quarterly frequency. This motivates us to employ a sample that includes the inflation spike and trough of the 1973–1975 recession and the inflation surge of the late 1970s, which are absent from the CPI-SPF, PCE-SPF, and Blue Chip Economic Indicators samples. See Nason and Smith (forthcoming) and our Online Supplementary Appendix (Mertens and Nason (2020)) for estimates obtained from data that omit the experience of the 1970s.

The structure of the paper follows. Section 2 builds a state space model in the observables of realized inflation and h-step ahead average SPF inflation predictions. We sketch the SMC methods used to estimate the state space models in Section 3. Results appear in Sections 4 and 5. Section 6 offers our conclusions.

2. Statistical and econometric models

Our paper considers a family of state space models that combine a statistical model of inflation and an economic model of forecast updating under sticky information. Inflation dynamics are represented by our extension of the SW-UC model. The economic model is the SI law of motion of inflation forecasts. Here, we describe a baseline version of our state space models, labeled $\mathcal{M}_0$, where the sticky-information weight is drifting, but the inflation gap persistence parameter is static. Alternative choices for which parameters are drifting or static are considered in Section 4 and in the Online Supplementary Appendix.

2.1 *A Stock and Watson UC model of inflation*

Stock and Watson (2007, 2016), Grassi and Proietti (2010), Creal (2012), Shephard (2015), Cogley and Sargent (2015), and Mertens (2016) estimated versions of the SW-UC model that decompose realized inflation, π_t, into trend inflation, τ_t, and gap inflation, $\tilde{\pi}_t$. These SW-UC models are nonlinear because stochastic volatility (SV) affects innovations to trend and gap. We enrich the SW-UC model by splitting the inflation gap into a persistent part, ε_t, that has stationary AR(1) dynamics, and a noise part $\zeta_{\pi,t}$. For parsimony, we endow the persistent, but not the irregular gap component, with stochastic volatility:

$$\pi_t = \tau_t + \tilde{\pi}_t, \tag{1}$$

$$\tilde{\pi}_t = \varepsilon_t + \sigma_{\zeta,\pi}\zeta_{\pi,t}, \quad \zeta_{\pi,t} \sim \mathcal{N}(0,1), \tag{2}$$

$$\tau_{t+1} = \tau_t + \varsigma_{\eta,t+1}\eta_t, \quad \eta_t \sim \mathcal{N}(0,1), \tag{3}$$

$$\varepsilon_{t+1} = \theta\varepsilon_t + \varsigma_{\upsilon,t+1}\upsilon_t, \quad \upsilon_t \sim \mathcal{N}(0,1), |\theta| < 1, \tag{4}$$

$$\ln \varsigma^2_{\ell,t+1} = \ln \varsigma^2_{\ell,t} + \sigma_\ell \xi_{\ell,t+1}, \quad \xi_{\ell,t+1} \sim \mathcal{N}(0,1), \ell = \eta, \upsilon, \tag{5}$$

where $\varsigma_{\eta,t}$, and $\varsigma_{\upsilon,t}$ denote stochastic volatility in the innovation η_t of τ_t, and stochastic volatility in the innovation υ_t of ε_t. Equations (1) and (2) decompose π_t into τ_t, ε_t, and $\zeta_{\pi,t}$. The random walk (3) describes the dynamics of τ_t, which also represents the Beveridge–Nelson trend of inflation in this model.[8] Persistence in ε_t is created with stationary AR(1) dynamics in equation (4) by restricting the static inflation gap persistence parameter $\theta \in (-1, 1)$. Equation (5) is a random walk in log-variances, $\ln \varsigma^2_{\eta,t+1}$ and $\ln \varsigma^2_{\upsilon,t+1}$, that generates SV in trend and gap inflation. We assume all shocks, $\zeta_{\pi,t}$, η_t, υ_t, $\xi_{\eta,t}$, and $\xi_{\upsilon,t}$ are mutually and serially uncorrelated.

[8]The relationship between UC models and the trend concept of Beveridge and Nelson (1981) is discussed, among others, by Watson (1986) and Morley, Nelson, and Zivot (2003); also see Nelson (2008).

2.2 *The sticky-information prediction mechanism of inflation*

Coibion and Gorodnichenko (2015) adapted the partial equilibrium model of sticky information by Mankiw and Reis (2002) to a setup in which agents' current forecast is their lagged sticky-information forecasts at static probability λ and with probability $1-\lambda$ their rational-expectations forecasts. Averaging across forecasters gives the h-step ahead sticky-information inflation prediction at time t, $\mathbf{F}_t\pi_{t+h}$, and the static probability λ is the sticky-information weight. Hence, $\mathbf{F}_t\pi_{t+h} = \lambda\mathbf{F}_{t-1}\pi_{t+h} + (1-\lambda)\mathbf{E}_t\pi_{t+h}$, which is a weighted average of the own lag, $\mathbf{F}_{t-1}\pi_{t+h}$, and a rational-expectations inflation forecast, $\mathbf{E}_t\pi_{t+h}$, $\lambda \in (0,1)$, and $h = 1,\ldots,\mathcal{H}$. In this environment, the sticky-information weight governs the average frequency, $1/(1-\lambda)$, at which $\mathbf{F}_t\pi_{t+h}$ is updated.

We innovate on a static sticky-information weight by investing λ with drift. An exogenous and bounded random walk drives time-variation in the sticky-information weight, where $\lambda_t \in (0,1)$ for all dates t. We interpret λ_t as summarizing beliefs the sticky-information forecaster holds about the underlying dynamics of inflation.

The sticky-information-SPF block is built around the SI law of motion of inflation forecasts with λ_t, its random walk, and a term structure of average SPF inflation predictions. The term structure links the average SPF participant's h-step ahead inflation predictions, $\pi^{\text{SPF}}_{t,t+h}$, to $\mathbf{F}_t\pi_{t+h}$ plus a classical measurement error, $\zeta_{h,t}$. These elements form the system of equations

$$\pi^{\text{SPF}}_{t,t+h} = \mathbf{F}_t\pi_{t+h} + \sigma_{\zeta,h}\zeta_{h,t}, \quad \zeta_{h,t} \sim \mathcal{N}(0,1), \tag{6}$$

$$\mathbf{F}_t\pi_{t+h} = \lambda_t\mathbf{F}_{t-1}\pi_{t+h} + (1-\lambda_t)\mathbf{E}_t\pi_{t+h}, \quad h = 1,\ldots,\mathcal{H}, \tag{7}$$

$$\lambda_{t+1} = \lambda_t + \sigma_\kappa\kappa_t, \quad \kappa_t \sim \mathcal{N}(0,1) \text{ s.t. } \lambda_{t+1} \in (0,1), \tag{8}$$

where h belongs to the set of positive integers, $h \in \mathbb{Z}^+$, and λ_{t+1} follows a bounded random walk with shocks drawn from a truncated normal that guarantees $\lambda_{t+1} \in (0,1)$.[9]

Equations (6)–(8) define the sticky-information prediction mechanism. Changes in λ_t and other state variables produce movements $\mathbf{F}_t\pi_{t+h}$ that create fluctuations in the observed term structure of SPF inflation predictions, $\pi^{\text{SPF}}_{t,t+h}$. The SPF term structure (6) includes measurement errors, $\zeta_{h,t}$, to capture deviations between $\pi^{\text{SPF}}_{t,t+h}$ and the sticky-information term structure of inflation, $\mathbf{F}_t\pi_{t+h}$, for $h = 1,\ldots,\mathcal{H}$. The SI law of motion (7) generates updates of $\mathbf{F}_t\pi_{t+h}$, for all h subject to drift in λ_t that is described by the random walk (8).

Updates of $\mathbf{F}_t\pi_{t+h}$ rely, in part, on $\mathbf{E}_t\pi_{t+h}$. We assume the average SPF participant computes $\mathbf{E}_t\pi_{t+h}$ using the SW-UC model of equations (1)–(5), where $\mathbf{E}_t\{\cdot\}$ conditions on the history of π_t, $\varsigma_{\eta,t}$, and $\varsigma_{\nu,t}$. Hence, the average SPF respondent knows the state variables of the SW-UC, τ_t, ε_t, $\varsigma_{\eta,t}$, and $\varsigma_{\nu,t}$. Nonetheless, we treat our SW-UC model as characterizing *reduced-form* inflation dynamics. While the SW-UC model is silent about the economic forces that may determine inflation—which, for example, might include an activity gap as in a Phillips curve—it has been shown to characterize the inflation process well, in particular for forecasting, as shown, among others, by Stock and Watson (2007, 2016), and Faust and Wright (2013).

[9] The innovations to λ_{t+1} are drawn from $\kappa_t \sim \mathcal{TN}(0,1;-\lambda_t/\sigma_\kappa,(1-\lambda_t)/\sigma_\kappa)$. $\mathcal{TN}(\mu,\sigma^2;\underline{x},\overline{x})$ denotes a truncated normal with support between $\underline{x}$ and $\overline{x}$, and mean and variance parameters μ and σ^2.

2.3 *A joint state space model of inflation and SPF forecasts*

This section presents our baseline state space model, $\mathcal{M}_0$. It is built on our SW-UC model of inflation, the SI law of motion of inflation forecasts, and a term structure of average SPF inflation predictions. Our SW-UC model yields a term structure of rational-expectations inflation forecasts. This term structure has a two factor representation driven by τ_t and ε_t. Similarly, we have sticky-information trend and persistent gap inflation, $\mathbf{F}_t\tau_t$ and $\mathbf{F}_t\varepsilon_t$, that are the factors of the term structure of sticky-information inflation forecasts.[10] The Online Supplemental Appendix shows that using a conjecture and verify procedure lets us construct state equations for $\mathbf{F}_t\tau_t$ and $\mathbf{F}_t\varepsilon_t$ that are driven by own lags and lags of τ_t and ε_t. The sticky-information states $\mathbf{F}_t\tau_t$ and $\mathbf{F}_t\varepsilon_t$ eliminate $\mathbf{F}_t\pi_{t+h}$ in the term structure equation (6) of $\pi^{\text{SPF}}_{t,t+h}$. The upshot is the term structure of rational-expectations inflation forecast places cross-equation restrictions on the rational-expectations and sticky-information state equations and the term structure of average SPF inflation predictions. The cross-equation restrictions show $\mathcal{M}_0$ is built on internally consistent rational expectations, sticky information, and average SPF inflation forecasts. The laws of motion of $\mathbf{F}_t\tau_t$ and $\mathbf{F}_t\varepsilon_t$ also depend crucially on the linearity of $\mathbf{E}_t\pi_{t+h}$ with respect to τ_t and ε_t and the linearity of $\mathbf{F}_t\pi_{t+h}$ with respect to $\mathbf{F}_t\tau_t$ and $\mathbf{F}_t\varepsilon_t$.

In our approach, the inflation process is characterized independently from the sticky-information prediction mechanism, which allows us to derive a simple recursive representation for the joint evolution of inflation and sticky-information forecasts. We begin with a state space representation of the SW-UC model. Rewrite the observation equation (1) as

$$\pi_t = \delta_{\mathcal{X}}\mathcal{X}_t + \sigma_{\zeta,\pi}\zeta_{\pi,t}, \tag{9}$$

where $\delta_{\mathcal{X}} = [1\ 1]$ and $\mathcal{X}_t = [\tau_t\ \varepsilon_t]'$. Stack the random walk (3) of τ_{t+1} on top of equation (4), which is the AR(1) of ε_{t+1}, to create the state equations of our SW-UC model

$$\mathcal{X}_{t+1} = \boldsymbol{\Theta}\mathcal{X}_t + \boldsymbol{\Upsilon}_{t+1}\mathcal{W}_t, \tag{10}$$

where $\boldsymbol{\Theta} = \left[\begin{smallmatrix} 1 & 0 \\ 0 & \theta \end{smallmatrix}\right]$, $\mathcal{W}_t = \left[\begin{smallmatrix} \eta_t \\ \nu_t \end{smallmatrix}\right]$, $\boldsymbol{\Upsilon}_{t+1} = \left[\begin{smallmatrix} \varsigma_{\eta,t+1} & 0 \\ 0 & \varsigma_{\nu,t+1} \end{smallmatrix}\right]$, and $\ln \varsigma^2_{\eta,t+1}$ and $\ln \varsigma^2_{\nu,t+1}$, are random walks as described by equation (5).

The SI law of motion (7) suggests a law of motion for the sticky-information states, $\mathbf{F}_t\mathcal{X}_{t+1} = \lambda_t\mathbf{F}_{t-1}\mathcal{X}_{t+1} + (1-\lambda_t)\mathbf{E}_t\mathcal{X}_{t+1}$, where $\mathbf{F}_t\mathcal{X}_t = [\mathbf{F}_t\tau_t\ \mathbf{F}_t\varepsilon_t]'$. We verify this conjecture in the Online Supplementary Appendix and generate the following recursive law of motion for the sticky-information forecast states:

$$\mathbf{F}_{t+1}\mathcal{X}_{t+1} = \lambda_{t+1}\boldsymbol{\Theta}\mathbf{F}_t\mathcal{X}_t + (1-\lambda_{t+1})\boldsymbol{\Theta}\mathcal{X}_t + (1-\lambda_{t+1})\boldsymbol{\Upsilon}_{t+1}\mathcal{W}_t. \tag{11}$$

The sticky-information state equations (11) inherits cross-equation restrictions from the SW-UC model's rational-expectations term structure of inflation forecasts in form of the transition and impulse matrices, $\boldsymbol{\Theta}$ and $\boldsymbol{\Upsilon}_{t+1}$ known from (10). In addition, as shown in

[10] Only the persistent gap component, ε_t matters for forecasting. For brevity, we will, hence, refer to ε_t simply as the gap component in this context.

the Online Supplementary Appendix, we can construct sticky-information forecasts for any horizon $h > 0$ as $\mathbf{F}_t\pi_{t+h} = \delta_{\mathcal{X}}\mathbf{F}_t\mathcal{X}_{t+h}$ with $\mathbf{F}_t\mathcal{X}_{t+h} = \boldsymbol{\Theta}^h\mathbf{F}_t\mathcal{X}_t$.[11]

The state equations of $\mathcal{M}_0$ are formed by stacking the state equations (10) of $\mathcal{X}_{t+1}$ on top of the sticky-information state equations (11)

$$\mathcal{S}_{t+1} = \boldsymbol{\mathcal{A}}_{t+1}\mathcal{S}_t + \boldsymbol{\mathcal{B}}_{t+1}\mathcal{W}_t, \tag{12}$$

where $\mathcal{S}_t = \begin{bmatrix} \mathcal{X}_t \\ \mathbf{F}_t\mathcal{X}_t \end{bmatrix}$, $\boldsymbol{\mathcal{A}}_{t+1} = \begin{bmatrix} \boldsymbol{\Theta} & \mathbf{0}_{2\times 2} \\ (1-\lambda_{t+1})\boldsymbol{\Theta} & \lambda_{t+1}\boldsymbol{\Theta} \end{bmatrix}$, $\boldsymbol{\mathcal{B}}_{t+1} = \begin{bmatrix} \boldsymbol{\Upsilon}_{t+1} \\ (1-\lambda_{t+1})\boldsymbol{\Upsilon}_{t+1} \end{bmatrix}$. Drift in the sticky-information weight and the stochastic volatilities creates nonlinearities in (12). However, the dynamics of $\mathcal{S}_t$ are linear conditional on a realization of

$$\mathcal{V}_t = [\varsigma_{\eta,t} \quad \varsigma_{\upsilon,t} \quad \lambda_t]'.$$

Accordingly, we will refer to $\mathcal{S}_t$ and $\mathcal{V}_t$ as linear and nonlinear states of the model. The state equations for the nonlinear states are given by (5) and (8). The parameter vector of the model is $\Psi = [\sigma_\eta^2\ \sigma_\upsilon^2\ \sigma_{\zeta,\pi}^2\ \sigma_{\zeta,1}^2\ \sigma_{\zeta,2}^2\ \sigma_{\zeta,4}^2\ \sigma_{\zeta,5}^2\ \sigma_\kappa^2\ \theta]'$.

We construct the observation equations of $\mathcal{M}_0$ using the observation equation (9) of our SW-UC model, SPF measurement equation (6), and rational-expectations and sticky-information term structures of inflation forecasts. These equations and term structures eliminate $\mathbf{F}_t\pi_{t+h}$ from the SPF term structure (6) giving us $\pi_{t,t+h}^{\text{SPF}} = \delta_{\mathcal{X}}\boldsymbol{\Theta}^h F_t\mathcal{X}_t + \sigma_{\zeta,h}\zeta_{h,t}$. Place these SPF term structure equations beneath the observation equation (9) of our SW-UC model to produce the observation equations of $\mathcal{M}_0$:

$$\mathcal{Y}_t = \boldsymbol{\mathcal{C}}\mathcal{S}_t + \boldsymbol{\mathcal{D}}\mathcal{U}_t, \tag{13}$$

where

$$\mathcal{Y}_t = \begin{bmatrix} \pi_t \\ \pi_{t,t+1}^{\text{SPF}} \\ \vdots \\ \pi_{t,t+\mathcal{H}}^{\text{SPF}} \end{bmatrix}, \qquad \boldsymbol{\mathcal{C}} = \begin{bmatrix} \delta_{\mathcal{X}} & \mathbf{0}_{1\times 2} \\ \mathbf{0}_{1\times 2} & \delta_{\mathcal{X}}\boldsymbol{\Theta} \\ \vdots & \vdots \\ \mathbf{0}_{1\times 2} & \delta_{\mathcal{X}}\boldsymbol{\Theta}^{\mathcal{H}} \end{bmatrix}, \qquad \boldsymbol{\mathcal{D}} = \begin{bmatrix} \sigma_{\zeta,\pi} & 0 & \dots & 0 \\ 0 & \sigma_{\zeta,1} & \dots & 0 \\ 0 & 0 & \ddots & 0 \\ 0 & 0 & \dots & \sigma_{\zeta,\mathcal{H}} \end{bmatrix},$$

$$\mathcal{U}_t = [\zeta_{\pi,t} \quad \zeta_{1,t} \quad \dots \quad \zeta_{\mathcal{H},t}]', \quad \text{and} \quad \boldsymbol{\Omega}_{\mathcal{U}} = \boldsymbol{\mathcal{D}}\boldsymbol{\mathcal{D}}'.$$

The observation equations (13) show the data, $\mathcal{Y}_t$, are linear in $\mathcal{S}_t$ in $\mathcal{M}_0$ with cross-equation restrictions imposed on the sticky-information forecasts that are inherited from the SW-UC model's rational-expectations inflation forecasts.

2.4 *Identification of the state space model*

Identification of our baseline state space model, $\mathcal{M}_0$, depends on term structures of rational-expectations and sticky-information inflation forecasts. The linear states, τ_t, ε_t, $\mathbf{F}_t\tau_t$, and $\mathbf{F}_t\varepsilon_t$, are identified on (i) a two-factor term structure of rational-expectations inflation forecasts produced by our SW-UC model, $\mathbf{E}_t\pi_{t+h} = \delta_{\mathcal{X}}\boldsymbol{\Theta}^h\mathcal{X}_t$, for $h = 1, \dots, \mathcal{H}$

[11] The sticky-information version of the broader inflation gap, $\tilde{\pi}_t$ defined in (2), follows as $\mathbf{F}_t\tilde{\pi}_t = \mathbf{F}_t\varepsilon_t + \sigma_{\zeta,\pi}$, $\mathbf{F}_t\zeta_{\pi,t}$ with $\mathbf{F}_t\varepsilon_t$ given by (11), and $\mathbf{F}_t\zeta_{\pi,t} = \lambda_t\zeta_{\pi,t}$, since $\zeta_{\pi,t}$ is serially uncorrelated.

and (ii) across the same forecast horizons, the term structure of average SPF inflation predictions, $\pi^{\text{SPF}}_{t,t+h} = \delta_{\mathcal{X}}\boldsymbol{\Theta}^h F_t\mathcal{X}_t + \sigma_{\zeta,h}\zeta_{h,t}$, that also has a two-factor representation. The state equations (12) imply that these factors, $\mathbf{F}_t\tau_t$ and $\mathbf{F}_t\varepsilon_t$, are each driven by a MA(∞) of τ_t and ε_t, respectively, where the MA coefficients reflect θ and the history of λ_t. Hence, information in the term structure of average SPF inflation predictions aids in identifying the level and slope of the term structures of rational-expectations and sticky-information inflation forecasts.

We use τ_t, $\mathbf{F}_t\tau_t$, ε_t, $\mathbf{F}_t\varepsilon_t$, and restrictions embedded in equations (12)–(13) of $\mathcal{M}_0$ to identify λ_t and θ. Intuition for the identification is developed by fixing the sticky-information weight, $\lambda_t = \lambda$. This assumption recovers the error correction mechanism, $\mathbf{F}_t\tau_t - \tau_t = \lambda(\mathbf{F}_{t-1}\tau_{t-1} - \tau_{t-1}) - \lambda\eta_t$, and common feature regression, $\mathbf{F}_t\varepsilon_t - \varepsilon_t = \lambda\theta(\mathbf{F}_{t-1}\varepsilon_{t-1} - \varepsilon_{t-1}) - \lambda\upsilon_t$, from the associated state space model.[12] The error correction mechanism identifies λ as its slope coefficient, which rests on the common trend restriction that cointegration places on $\mathbf{F}_t\tau_t$ and τ_t. Once λ is known, θ is identified in the common feature regression because $\mathbf{F}_t\varepsilon_t$ and ε_t share a common cycle.[13]

The Online Supplementary Appendix provides a more detailed analysis of the identification issue, based on results in Harvey (1991) and Komunjer and Ng (2011).

3. Econometric methods

This section summarizes the SMC filtering and smoothing algorithms used to estimate our state space models. Although we illustrate the problems of particle filtering and learning in the context of our baseline model $\mathcal{M}_0$, our description here is fairly generic and applies also to other model variants that are presented in Section 4. Our state space models differ in whether the sticky-information weight, λ_t, or the gap-persistence parameter, θ (or both), are treated as drifting or static. All model variants have the same linear states (as described in Section 2) and include stochastic volatilities among the nonlinear states. A more detailed account of our SMC methods is provided in the Online Supplementary Appendix.

We estimate states and static parameters of our state space models with SMC methods proposed by Carvalho et al. (2010) and refined by Lopes and Tsay (2011).[14] This class

[12] Grant and Thomas (1999) argued weak forms of forecast efficiency demand that survey errors are stationary and independent of whether surveys provide optimal and efficient predictions of inflation. An equivalent restriction is surveys of inflation forecasts and realized inflation cointegrate. Kozicki and Tinsley (2012), Mertens (2016), and Nason and Smith (forthcoming) applied this restriction to generate estimates of trend inflation from samples of realized inflation and surveys of inflation forecasts.

[13] Jain (2019) used forecast revisions to identify predictability of individual SPF inflation forecasts. Applying Jain's approach to our state space model, and neglecting measurement error, sets $\theta = (\mathbf{F}_t\pi_{t+h+2} - \mathbf{F}_t\pi_{t+h})/(\mathbf{F}_t\pi_{t+h+1} - \mathbf{F}_t\pi_{t+h})$. Given θ, the level and slope of the term structure of sticky-information inflation forecasts are identified by $\mathbf{F}_t\pi_{t+h}$ and two adjacent forecasts. Krane (2011) used a similar approach, but identifies permanent and transitory components in revisions to the term structure of Blue Chip forecasts.

[14] A state space model can be estimated by wrapping a Markov chain Monte Carlo (MCMC) sampler around a particle filter. Andrieu, Doucet, and Holenstein (2010) gave particle MCMC (PMCMC) theoretical foundations. Schorfheide, Song, and Yaron (2018) put a PMCMC sampler into practice. A PMCMC algorithm can engender large computational costs because it runs a simulation inside a simulation.

of SMC methods is known as particle learning. Particle learning jointly filters the states, $\mathcal{S}_t$ and $\mathcal{V}_t$, and static parameters, Ψ, of a state space model for every date $t = 1, \ldots, T$. The result is a sequence of filtered estimates of states *and parameters* that condition only on time t information, which mimics the real-time character of the SPF data.

When a state space model is nonlinear and/or non-Gaussian, direct sampling from the posterior distribution of the states is often impossible. A particle filter builds on the idea of sequential importance sampling, where inference is based on simulating proposed sequences for the states, which are then weighted by their likelihood ratios between target and proposal distribution. Particle filtering provides inference about latent states for given parameter values. Carvalho et al. (2010) combined inference on the states with online estimation of a model's parameters in a particle learning filter.

Particle learning relies on sufficient statistics to efficiently construct the posterior of a state space model. Sufficient statistics are tied to prior beliefs about the state space model and its dynamic structure. We place priors on Ψ that are conjugate. Conjugate priors yield analytic solutions that serve as laws of motion to update sufficient statistics of Ψ, which are coefficients of its priors. Filtered estimates of Ψ are drawn from particle streams of the sufficient statistics. The result is an online process that learns about Ψ by moving through the sample date by date.

Carvalho et al. (2010) advised, if feasible, to Rao–Blackwellize a state space model. Rao–Blackwellization exploits the conditionally linear and Gaussian dynamics of $\mathcal{S}_t$, given $\mathcal{V}_t$ and Ψ. (Hence, we refer to $\mathcal{S}_t$ and $\mathcal{V}_t$ as the "linear" and "nonlinear" states.) For a Rao–Blackwellized state space model, the Kalman filter analytically marginalizes out $\mathcal{S}_t$ and tracks its sufficient statistics while inference about the nonlinear states is still left to importance sampling methods. The use of analytic inference steps over Monte Carlo methods, wherever possible, lowers the sampling error of the particle learning filter, thus improving its efficiency.

We estimate the smoothed states of our Rao–Blackwellized state space models using an algorithm created by Lindsten et al. (2016). Their smoothing algorithm accounts for Rao–Blackwellization of a state space model by first forward filtering (i.e., using a particle learning filter) of all the states, backward smoothing of the nonlinear states, and forward smoothing of the linear states. We revise the Rao–Blackwellized particle smoother to marginalize out the sample uncertainty induced by estimating the static parameters with the particle learning filter.

3.1 *Particle filters and particle learning*

Here, we illustrate the problems of particle filtering and learning in the context of our baseline model $\mathcal{M}_0$. Later in this section, we describe how to compute a model's marginal data density from output of the particle learning filter, and the construction of smoothed estimates of the model's states.

A Rao–Blackwellized bootstrap filter For known parameters values Ψ, the state and observation equations of our model yield a recursive nonlinear state space model of the

following form:[15]

$$\mathcal{Y}_t \sim p(\mathcal{Y}_t|\mathcal{S}_t, \mathcal{V}_t; \Psi),$$

$$\mathcal{S}_t, \mathcal{V}_t \sim p(\mathcal{S}_t, \mathcal{V}_t|\mathcal{S}_{t-1}, \mathcal{V}_{t-1}; \Psi) \tag{14}$$

$$= p(\mathcal{S}_t, |\mathcal{V}_t, \mathcal{S}_{t-1}; \Psi) \cdot p(\mathcal{V}_t|\mathcal{V}_{t-1}; \Psi) \tag{15}$$

Importantly, $p(\mathcal{S}_t, |\mathcal{V}_t, \mathcal{S}_{t-1}; \Psi)$ and $p(\mathcal{Y}_t|\mathcal{S}_t, \mathcal{V}_t; \Psi)$ are joint normals and the state transition density can be factorized as in (15), which gives the model a conditionally linear structure.

In general, a particle filter approximates the posterior density of the states with a finite set of M realizations for the states, $\{\mathcal{S}_t^{(i)}, \mathcal{V}_t^{(i)}\}_{i=1}^M$, that are also known as "particles," and a set of importance sampling weights $w_t^{(i)} \in (0, 1)$, $i = 1, \ldots, M$.[16] A simple, albeit brute force method is the bootstrap filter, which sequentially generates proposals for the states from their prior in (14).[17] Given such a set of proposed particles, the weights are constructed from each particle's likelihood $w_t^{(i)} \propto p(\mathcal{Y}_t|\mathcal{S}_t^{(i)}, \mathcal{V}_t^{(i)}; \Psi)$. However, the bootstrap filter is not an efficient SMC method. In general, the bootstrapped proposals neglect information from the data about high-likelihood regions for the states; to remedy this defect, we wrap our inference inside an auxiliary particle filter described further below. Moreover, bootstrapping proposals for nonlinear *and linear* states ignores conditional linearity of our state space model.

Rao–Blackwellization recognizes that inference about the linear states can be performed with standard Kalman filtering formulas when conditioning on a given history of the non-linear states. Chen and Liu (2000) combined such Rao–Blackwellization for the linear states with sequential importance sampling of the nonlinear states to represent the joint posterior of linear and nonlinear states with a mixture of Kalman filters.

The conditional linearity of the state space implies that, conditional on particle i's history of the nonlinear states, $\mathcal{V}^{t,(i)}$, the posterior of $\mathcal{S}_t$ is a multivariate normal that is fully characterized by two sufficient statistics:

$$\mathcal{S}_{t|t}^{(i)} = \mathbf{E}\big(\mathcal{S}_t|\mathcal{Y}^t; \mathcal{V}^{t,(i)}, \Psi\big) \quad \text{and} \quad \Sigma_{t|t}^{(i)} = \mathbf{Var}\big(\mathcal{S}_t|\mathcal{Y}^t; \mathcal{V}^{t,(i)}, \Psi\big).$$

The Kalman filter provides recursions for $\mathcal{S}_{t|t}^{(i)}$ and $\Sigma_{t|t}^{(i)}$ as well as the prediction error decomposition of the likelihood, $p(\mathcal{Y}^t|\mathcal{V}_t^{(i)}; \Psi)$; as described below, the latter matters for calculating the importance weights of the particles. Details are provided in the Online Supplementary Appendix.

Rao–Blackwellization lowers sampling error in the particle learning filter by marginalizing out $\mathcal{S}_t$ analytically with the Kalman filter. While Rao–Blackwellization can be applied to the linear states, we generate proposals for the nonlinear states from their prior shown in (15). However, in contrast to a simple bootstrap as outlined above, our proposals are adapted to the observed data, $\mathcal{Y}^t$, by use of an auxiliary particle filtering step that is described next.

[15] State and measurement equations of $\mathcal{M}_0$ are given by (5), (8), (12), and (13).

[16] $\mathcal{Y}^t$ denotes the history of observations $\mathcal{Y}^t = \{\mathcal{Y}_1, \mathcal{Y}_2, \ldots, \mathcal{Y}_t\}$.

[17] Originally proposed by Gordon, Salmond, and Smith (1993), the bootstrap filter combines sequential importance sampling and resampling with replacement to consistently estimate the states.

Proposal densities, resampling, and propagation SMC methods need a proposal density to create a particle stream of the states that is not "too far" from the true posterior. We focus our discussion on proposals for the nonlinear states, $\mathcal{V}_t$ since the linear states will be Rao–Blackwellized.

Bootstrap proposals of $\mathcal{V}_t$ for the ith particle could be generated by drawing from $p(\mathcal{V}_t|\mathcal{V}_{t-1}^{(i)};\Psi)$. An alternative is the auxiliary particle filter (APF) of Pitt and Shephard (1999, 2001) that seeks to adapt the proposal to the data, $\mathcal{Y}^t$, for greater efficiency. We follow Carvalho et al. (2010), and embed ideas from the APF in a particle learning filter. Before turning to the specifics of online parameter estimation with particle learning, we outline the APF elements of the filter.

Ideally, we would like to draw proposals from $p(\mathcal{V}_t|\mathcal{Y}_t, \mathcal{S}_{t-1|t-1}^{(i)}, \Sigma_{t-1|t-1}^{(i)}, \mathcal{V}_{t-1}^{(i)};\Psi)$. However, in our case, it is not possible to draw directly from such a fully adapted proposal density, due to the nolinearities induced by $\mathcal{V}_t$ into the model. Instead, we combine bootstrap proposals with a two-stage weighting scheme, described among others by Pitt, dos Santos Silva, Giordani, and Kohn (2012) that refines the original APF of Pitt and Shephard (1999).[18]

The APF two-stage scheme seeks to reweigh the time $t-1$ particle swarm toward higher-likelihood regions at t before propagating the particles. Specifically, consider the filtering problem at t based on a swarm of particles inherited from time $t-1$ with importance weights proportional to $w_{t-1}^{(i)}$ for $i=1,\ldots,M$. The two-stage scheme consists of a first set of weights, $w_{t|t-1}^{(i)}$, that reflects the product of $W_{t-1}^{(i)}$ and the time t likelihood of each particle obtained under the assumption that $V_t^{(i)}$ would remain identical to $V_{t-1}^{(i)}$.[19] The time $t-1$ particles, $V_{t-1}^{(i)}$, $\mathcal{S}_{t-1|t-1}^{(i)}$, and $\Sigma_{t-1|t-1}^{(i)}$ are then resampled in proportion to $w_{t|t-1}^{(i)}$ before propagating the nonlinear states with draws from $p(\mathcal{V}_t|\mathcal{V}_{t-1}^{(i)};\Psi)$. Conditioning the first-stage weights $w_{t-1|t}^{(i)}$ on $\mathcal{Y}_t$ seeks to propagate time t particles that carry greater weight in the likelihood, which yields potentially more efficient estimates of the states.[20]

The final step computes a second set of weights, denoted $w_t^{(i)}$, that reflects the ratio of likelihoods attained by each particle i before and after the propagation step. The normalized second-stage weights $W_t^{(i)} = w_t^{(i)}/\sum_i w_t^{(i)}$ serve as importance weights to calculate estimates of the nonlinear states $\mathcal{V}_{t|t} = \sum_i W_t^{(i)}\mathcal{V}_t^{(i)}$ and other objects of interest. As described further below, the two-stage weights, $w_{t-1|t}^{(i)}$ and $w_t^{(i)}$, are involved in calculating the model's marginal data density.

[18]The key refinement is to omit the second resampling step of Pitt and Shephard (1999), which would otherwise increase Monte Carlo error. Similar versions of such second-generation APF are presented, among others, by Johansen and Doucet (2008) and Herbst and Schorfheide (2016).

[19]Given the random-walk properties of the nonlinear states, our first-stage assumption of unchanged $\mathcal{V}_t$ corresponds to Pitt and Shephard's proposal to propagate first-stage particles according to their median predictions.

[20]Resampling before propagation of the states mitigates particle degeneracy by conditioning $w_{t-1|t}^{(i)}$ on $\mathcal{Y}_t$. Particle degeneracy occurs when a few particles carry most of the weight at future filtering steps. The result is unevenly distributed weights implying inadequate coverage of regions of high likelihood, which the APF aims to fix. However, Johansen and Doucet (2008) and Herbst and Schorfheide (2016) noted the efficacy of the APF rests on the initial proposal having fatter tails than the target.

Parameter inference with particle learning We embed Rao–Blackwellization and APF steps in a particle learning filter.[21] A naive approach to online estimation would be to include an initial set of proposals for the static parameters in the particle stream. However, absent a propagation equation for the static parameters, successive resampling of the particles of Ψ would collapse the stream onto only a few particles. The result would be a poor approximation of the posterior of Ψ.

Particle learning solves the problem of particle degeneracy by tracking each particle's posterior *distribution* for Ψ instead of a mere proposal for its realized value.[22] Tracking posteriors for Ψ is tractable when the distribution can be represented by sufficient statistics, which is feasible in the case of conjugate priors. To that end, we place conjugate priors on the static parameters.

Since the priors of the static parameters are conjugate, the posterior distributions are analytic; moreover, priors and posteriors are represented by a common set of sufficient statistics. This insight suggests laws of motion for parameters of the posterior distributions in terms of updating equations for their sufficient statistics. For example, given an inverse-gamma prior for the volatility of shocks to trend SV, $\sigma_\eta^2 \sim \mathcal{IG}(\alpha_{t-1}^{(i)}/2, \beta_{\eta,t-1}^{(i)}/2)$, its posterior distribution is also an inverse gamma with updated scale and shape parameters $\alpha_t^{(i)} = \alpha_{t-1}^{(i)} + 1$ and $\beta_{\eta,t}^{(i)} = \beta_{\eta,t-1}^{(i)} + \Delta \ln \varsigma_{\eta,t}^{2,(i)}$.

All told, similar to Rao–Blackwellization of $\mathcal{S}_t$, we represent the posterior distribution of Ψ by a vector of sufficient statistics, denoted Γ. At a given point in time t, the ith particle tracks sufficient statistics for posterior of the parameters, denoted $\Gamma_t^{(i)}$, alongside $\mathcal{S}_{t|t}^{(i)}$, $\Sigma_{t|t}^{(i)}$, $\mathcal{V}_t^{(i)}$. In response to new data, Γ gets updated analytically as illustrated above, and the particle learning filter tracks a system of such updating equations for the sufficient statistics: $\Gamma_t^{(i)} = f(\Gamma_{t-1}^{(i)}, \mathcal{V}_t^{(i)}, \mathcal{V}_{t-1}^{(i)}, \mathcal{S}_t^{(i)}, \mathcal{Y}^t)$, where $\mathcal{S}_t^{(i)} \sim \mathcal{N}(\mathcal{S}_{t|t}^{(i)}, \Sigma_{t|t}^{(i)})$, and further details provided in the Online Supplementary Appendix.

The conditional posterior for the parameters obtained at date t, represented by $\Gamma_t^{(i)}$, becomes the prior for parameter inference at time $t+1$. Subsequent to propagating the sufficient statistics to $\Gamma_t^{(i)}$, we draw M particles of the static parameters from $\Psi^{(i)} \sim p(\Psi|\Gamma_{t+1}^{(i)})$. These particle draws, $\Psi^{(i)}$, are then used by the Rao–Blackwellized APF outlined above to filter the $t+1$ states. As a result, the particle learning filter generates posteriors of the states that fully reflect parameter uncertainty.

3.2 *Estimating the marginal data density*

The likelihood of our state space models is computed in the particle learning filter. The marginal data density (MDD), $p(\mathcal{Y}_t)$, is based on techniques described by Pitt et al. (2012, Appendix A.2). They compute the time t contributions to the MDD of a state space

[21] Early examples of particle learning are Liu and West (2001), Djuric and Miguez (2002), Fearnhead (2002), and Storvik (2002). Särkkä (2013) has a useful summary of particle learning. Our particle learning filter is grounded in algorithm 7 of Lopes and Tsay (2011).

[22] The relevant posteriors for Ψ are conditional on each particle's history of the states. For brevity, we will henceforth refer to these posteriors without explicit reference to this conditionality.

model using the cloud of first- and second-stage weights, $\{w_{t-1|t}^{(i)}, w_t^{(i)}\}_{i=1}^M$ as follows:

$$p(\mathcal{Y}_t|\mathcal{Y}^{t-1}) = \left[\frac{1}{M}\sum_{i=1}^{M} w_t^{(i)}\right]\sum_{i=1}^{M} w_{t-1|t}^{(i)}. \tag{16}$$

In Section 4, we employ MDDs constructed from equation (16) to assess our baseline state space model against three alternative state space models.

3.3 *A Rao–Blackwellized particle smoother*

Rao–Blackwellization is not costless. Conditionally, linear states create problems for particle smoothing algorithms that merge forward filtering with backward simulation of particles drawn from $p(\mathcal{S}_t, \mathcal{V}_t|\mathcal{Y}^T, \Psi)$ as, for example, in Godsill, Doucet, and West (2004). This class of particle smoothers is known as forward-filtering with backward-simulation (FFBS).[23] A FFBS algorithm is a recursive decomposition of the posterior of the smoothed states that rely on Markovian state dynamics. However, this decomposition is unsuited for a conditionally linear state space model, when Rao–Blackwellization of the linear states has been applied in the filtering step. The problem is that after marginalizing out $\mathcal{S}_t$, the posterior of $\mathcal{V}_t$ is not Markovian anymore.

Lindsten et al. (2016) proposed a Rao–Blackwellized particle smoother to solve the problem. Their particle smoother extends the FFBS procedures of Godsill, Doucet, and West (2004) to a Rao–Blackwellized state space model by forward filtering of the linear and nonlinear states, backward smoothing of the nonlinear states, and forward smoothing of the linear states conditional on the smoothed nonlinear states. Hence, Lindsten et al. (2016) call their algorithm a forward-backward-forward smoother.

We assign the initial forward filtering step of the Lindsten et al. (2016) particle smoother to our Rao–Blackwellized particle learning filter. This produces the joint posterior of $\mathcal{S}_t$ and $\mathcal{V}_t$, $p(\mathcal{S}_t, \mathcal{V}_t|\mathcal{Y}^t, \Psi)$, for a given realization of the parameter vector Ψ. After summarizing the approach of Lindsten et al. (2016) for generating smoothed draws of the states for a given parameter vector, we describe how we integrate out uncertainty over the parameter vector.

The backward smoothing step rests on the decomposition of the target density of the nonlinear states, $p(\mathcal{V}^T|\mathcal{Y}^T, \Psi)$, into $p(\mathcal{V}^t|\mathcal{V}^{t+1}, \mathcal{Y}^T, \Psi)p(\mathcal{V}^{t+1:T}|\mathcal{Y}^T, \Psi)$. However, Lindsten et al. (2016) initialize their Rao–Blackwellized particle smoother at date T by sampling from the filtered nonlinear states, $\{\mathcal{V}_T^{(i)}\}_{i=1}^M$, to obtain smoothed nonlinear states, $\{\widetilde{\mathcal{V}}_T^{(i)}\}_{i=1}^M$. The factorization of $p(\mathcal{V}^T|\mathcal{Y}^T, \Psi)$ is useful in smoothing backwards because $p(\mathcal{V}^t|\mathcal{V}^{t+1}, \mathcal{Y}^T, \Psi)$ has information about the probabilities needed to draw $\{\widetilde{\mathcal{V}}_t^{(i)}\}_{i=1}^M$ from $\{\mathcal{V}_t^{(i)}\}_{i=1}^M$. Since $p(\mathcal{V}^t|\mathcal{V}^{t+1}, \mathcal{Y}^T, \Psi)$ is expensive to compute, Lindsten et al. (2016) pro-

[23] Godsill, Doucet, and West (2004) is a classic example of a particle smoother built on FFBS methods. Carvalho et al. (2010) and Lopes and Tsay (2011) apply FFBS methods to particle learning filters.

posed a simulator to backward filter the nonlinear states.[24] The simulator relies on the decomposition $p(\mathcal{V}^t|\mathcal{V}^{t+1},\mathcal{Y}^T,\Psi)\propto p(\mathcal{Y}^{t+1:T},\mathcal{V}^{t+1:T}|\mathcal{V}^t,\mathcal{Y}^t,\Psi)\,p(\mathcal{V}^t|\mathcal{Y}^t,\Psi)$

The third step of the Rao–Blackwellized particle smoother runs the Kalman filter forward to generate smoothed estimates of $\mathcal{S}_t$ and Σ_t by drawing from $p(\mathcal{S}_t|\widetilde{\mathcal{V}}^t,\mathcal{Y}^t,\Psi)$. These are the sufficient statistics of $\widetilde{\mathcal{S}}_t$ employed in simulations to approximate the predictive density $p(\mathcal{Y}^{t+1:T},\mathcal{V}^{t+1:T}|\mathcal{V}^t,\mathcal{Y}^t,\Psi)$. Although $p(\mathcal{V}^t|\widetilde{\mathcal{V}}^{t+1},\mathcal{Y}^T,\Psi)$ does not condition on $\widetilde{\mathcal{S}}_t$, its estimates are needed to compute the probability of sampling $\widetilde{\mathcal{V}}^{t:T}$.

Finally, given the ability to draw smoothed trajectories $\mathcal{V}^T$ and $\mathcal{S}^T$ conditional on parameters we integrate out uncertainty over the parameter vector according to

$$p\big(\mathcal{V}^T,\mathcal{S}^T|\mathcal{Y}^T\big)=\int_{\Psi}p\big(\mathcal{V}^T,\mathcal{S}^T|\mathcal{Y}^T,\Psi\big)p\big(\Psi|\mathcal{Y}^T\big)\,d\Psi,$$

where we use draws of Ψ obtained from the particle learning filter in repeated calls to the smoother of Lindsten et al. (2016). Further details are described in the Online Supplmentary Appendix.

4. The model space, priors, data, and estimates

This section presents our alternative state space models, priors, data sources, and estimates from the state space models. The different models are evaluated based on the first implied by the marginal data density. We present estimates of filtered and smoothed states, and static parameters for the state space model favored by the data and select alternatives. A more exhaustive set of results can be found in the Online Supplementary Appendix.

4.1 *The model space*

We evaluate our baseline state space model, $\mathcal{M}_0$, against three alternative specification. The alternative models differ in whether the inflation gap persistence parameter or the sticky-information weight (or both) are static or drifting, and the Online Supplementary Appendix derives the resulting state and observation equations for each model variant.[25] All four models feature stochastic volatility in trend and gap inflation.

The first alternative state space model, $\mathcal{M}_1$, fixes the inflation gap persistence parameter and sticky-information weight, $\theta_t=\theta$ and $\lambda_t=\lambda$. Letting both parameters drift defines the second alternative state space model, $\mathcal{M}_2$. Drift in the inflation gap persistence parameter evolves as a bounded random walk $\theta_{t+1}=\theta_t+\sigma_\phi\phi_t$, where innovations are drawn from a truncated normal, $\phi_t\sim\mathcal{TN}(0,1;(-1-\theta_t)/\sigma_\phi,(1-\theta_t)/\sigma_\phi)$ to ensure that θ_t remains inside the unit circle. The third alternative state space model, $\mathcal{M}_3$, holds λ fixed while the inflation gap persistence parameter drifts, θ_t.

[24]The Kalman filter creates an exact predictive density (up to a normalizing constant). However, computing the density involves running the Kalman filter across M particle streams while iterating it forward from the start of the sample to date T. These calculations are computationally costly, which motivate Lindsten et al. (2016) to approximate the predictive density with simulated sufficient statistics.

[25]We thank the editor and referees for suggesting the model space be expanded as shown in Table 1.

TABLE 1. List of baseline and alternative state space models.

	λ	
θ	Time-Varying	Constant
Constant	$\mathcal{M}_0$	$\mathcal{M}_1$
Time-varying	$\mathcal{M}_2$	$\mathcal{M}_3$

Our alternative state space models imply different compositions of the parameter vector, Ψ, and the vector of nonlinear states, $\mathcal{V}_t$, which are henceforth distinguished as Ψ_i and $\mathcal{V}_{i,t}$ for $i = 0, 1, 2, 3$. The baseline model has three nonlinear states in $\mathcal{V}_{0,t} = [\varsigma_{\eta,t}\ \varsigma_{\upsilon,t}\ \lambda_t]'$. For $\mathcal{M}_1$, stochastic volatilities are the only nonlinear states, $\mathcal{V}_{1,t} = [\varsigma_{\eta,t}\ \varsigma_{\upsilon,t}]'$. For $\mathcal{M}_2$ and $\mathcal{M}_3$, the nonlinear state vectors are $\mathcal{V}_{2,t} = [\varsigma_{\eta,t}\ \varsigma_{\upsilon,t}\ \theta_t\lambda_t]'$ and $\mathcal{V}_{3,t} = [\varsigma_{\eta,t}\ \varsigma_{\upsilon,t}\ \theta_t]'$. The Online Supplementary Appendix provides further details.

4.2 *Priors and initial conditions*

This section describes our priors on the static parameters of $\mathcal{M}_0$, $\mathcal{M}_1$, $\mathcal{M}_2$, and $\mathcal{M}_3$. Restrictions on the state space models imply the static parameter vectors Ψ_0, Ψ_1, Ψ_2, and Ψ_3 differ, but the state space models share many static parameters in common. For example, replace σ_κ^2 with λ in $\mathcal{M}_1$ to produce $\Psi_1 = [\sigma_\eta^2\ \sigma_\upsilon^2\ \sigma_{\zeta,\pi}^2\ \sigma_{\zeta,1}^2\ \sigma_{\zeta,2}^2\ \sigma_{\zeta,3}^2\ \sigma_{\zeta,4}^2\ \sigma_{\zeta,5}^2\ \lambda\ \theta]'$ that otherwise is identical to $\Psi_0 = [\sigma_\eta^2\ \sigma_\upsilon^2\ \sigma_{\zeta,\pi}^2\ \sigma_{\zeta,1}^2\ \sigma_{\zeta,2}^2\ \sigma_{\zeta,3}^2\ \sigma_{\zeta,4}^2\ \sigma_{\zeta,5}^2\ \sigma_\kappa^2\ \theta]'$. Drifting inflation gap persistence parameter and sticky-information weight in $\mathcal{M}_2$ yield $\Psi_2 = [\sigma_\eta^2\ \sigma_\upsilon^2\ \sigma_{\zeta,\pi}^2\ \sigma_{\zeta,1}^2\ \sigma_{\zeta,2}^2\ \sigma_{\zeta,3}^2\ \sigma_{\zeta,4}^2\ \sigma_{\zeta,5}^2\ \sigma_\kappa^2\ \sigma_\phi^2]'$ that equals Ψ_0 up to substituting σ_ϕ^2 for θ. Finally, swap drift in the sticky-information weight for drift in the inflation gap persistence parameter in $\mathcal{M}_3$ to set $\Psi_3 = [\sigma_\eta^2\ \sigma_\upsilon^2\ \sigma_{\zeta,\pi}^2\ \sigma_{\zeta,1}^2\ \sigma_{\zeta,2}^2\ \sigma_{\zeta,3}^2\ \sigma_{\zeta,4}^2\ \sigma_{\zeta,5}^2\ \lambda\ \sigma_\phi^2]'$.

We posit priors for the static volatility parameters and initial conditions of θ_t, λ_t, $\mathcal{S}_t$, and $\mathcal{V}_{k,t}$, $k = 0, 1, 2,$ and 3. The scale volatility parameters on the stochastic volatilities, random walks of θ_t and λ_t, and measurement errors are given inverse gamma ($\mathcal{IG}$) priors. Table 2 reports the scale and shape parameters, α_ℓ and β_ℓ, of the $\mathcal{IG}$ priors along with the implied prior means, 5% and 95% quantiles.

Several features of our priors are worth discussing. First, we center the priors of σ_η^2 and σ_υ^2 around the fixed coefficient values used by Stock and Watson (2007). Next, the prior mean of 0.01 assigned to σ_κ^2 is smaller reflecting the bounded support of λ_t. Nonetheless, this prior admits substantial variation in λ_t between the bounds of zero and one when estimating $\mathcal{M}_0$ and $\mathcal{M}_2$. For similar reasons, the prior for the volatility of shocks to inflation gap persistence, σ_ϕ^2, in $\mathcal{M}_2$ and $\mathcal{M}_3$, has been centered around a value of 0.01. Second, our priors on σ_η^2 and σ_υ^2 deliver quantiles that exhibit greater variation compared with σ_ϕ^2 and σ_κ^2. Third, the quantiles of $\sigma_{\zeta,\pi}^2, \sigma_{\zeta,1}^2, \ldots, \sigma_{\zeta,5}^2$ depict our belief that the irregular component of π_t and measurement errors in $\pi_{t,t+h}^{\text{SPF}}$ are volatile.

Table 3 lists our priors for the cases where inflation gap persistence, θ, or the sticky-information weight, λ are static parameters. The priors obey $\theta \in (-1, 1)$ and $\lambda \in (0, 1)$. For $\mathcal{M}_0$, and $\mathcal{M}_1$, we endow θ with a truncated standard normal prior. This prior has 5%

TABLE 2. Priors on the scale volatility parameters.

Scale Volatility on Innovation to		α_ℓ	β_ℓ	Mean	Quantiles 5% 95%
Trend inflation SV, $\ln \varsigma_{\eta,t+1}$:	σ_η^2	3.0	0.04	0.04	[0.005, 0.114]
Gap inflation SV, $\ln \varsigma_{\upsilon,t+1}$:	σ_υ^2	3.0	0.04	0.04	[0.005, 0.114]
TVP-AR1 coefficient, θ_{t+1}:	σ_ϕ^2	3.0	0.01	0.01	[0.001, 0.028]
Sticky-information weight, λ_{t+1}:	σ_κ^2	3.0	0.01	0.01	[0.001, 0.028]
Irregular noise component in π_t:	$\sigma_{\zeta,\pi}^2$	20.0	1.80	0.10	[0.057, 0.166]
Measurement error on $\pi_{t,t+h}^{\text{SPF}}$:	$\sigma_{\zeta,h}^2$	20.0	1.80	0.10	[0.057, 0.166]

Note: Priors on the static volatility parameters are $\sigma_\ell^2 \sim \mathcal{IG}(\alpha_\ell/2, \beta_\ell/2)$, where $\ell = \eta, \upsilon, \kappa, \zeta_\pi$, and ζ_h for $h = 1, \ldots, 5$. For $\alpha_\ell > 2$, the mean of the $\mathcal{IG}$ distribution is $\beta_\ell/(\alpha_\ell - 1)$. The priors for σ_ϕ^2 and σ_κ^2 listed above apply only for models where θ and λ (or both) are drifting parameters.

and 95% quantiles at -0.87 and 0.87. For $\mathcal{M}_1$, and $\mathcal{M}_3$, the beta prior for λ has shape parameters of unity and is thus equivalent to the uniform distribution on the unit interval. In essence, we have noninformative priors over θ and λ.

Priors on the initial conditions of the linear and nonlinear states appear in Table 4. The left side of the table lists priors on the initial conditions of the linear states, τ_0, ε_0, $\mathbf{F}_0\tau_0$, and $\mathbf{F}_0\varepsilon_0$. Initial conditions on the stochastic volatilities, $\ln \varsigma_{\eta,0}^2$ and $\ln \varsigma_{\upsilon,0}^2$, drifting sticky-information weight, λ_0, and drifting inflation gap parameter, θ_0, are found on the right side of the Table 4. We draw τ_0 and $\mathbf{F}_0\tau_0$ from normal priors. The prior means are 2%, which is about the mean of GNP deflator inflation on a $1958Q1$ to $1967Q4$ training sample. A variance of 100^2 yields an approximately flat prior over the relevant range of values for τ_0 and $\mathbf{F}_0\tau_0$ in post-war U.S. data. The joint prior of ε_0 and $\mathbf{F}_0\varepsilon_0$ is drawn from the ergodic bivariate normal distribution $\mathcal{N}(\mathbf{0}_{2\times 1}, \boldsymbol{\Sigma}_{\varepsilon,0})$ as implied by the particle draws for initial levels of the nonlinear states; see the notes to Table 4.

The last column of Table 4 display our priors on initial conditions of the nonlinear states. We endow priors of $\ln \varsigma_{\upsilon,0}^2$ and $\ln \varsigma_{\eta,0}^2$ with normal distributions. Prior means are calibrated to pre-1968 inflation data similar to Stock and Watson (2007). Large variances reflect prior uncertainty about $\ln \varsigma_{\upsilon,0}^2$ and $\ln \varsigma_{\eta,0}^2$. Table 4 also shows that the priors on the initial conditions for θ_0 and λ_0 are fairly uninformative.

TABLE 3. Priors on static-parameter versions θ and λ.

		Distribution	Mean	STD	Quantiles 5% 95%
Gap inflation AR(1):	θ	$\mathcal{TN}(0, 1; -1, 1)$	0.0	1.0	$[-0.87, 0.87]$
Sticky-information weight:	λ	Beta(1, 1)	0.5	–	[0.05, 0.95]

Note: The above-listed priors pertain to versions of our state space models where θ or λ (or both) are static parameters. $\mathcal{TN}(0, 1; -1, 1)$ represents a truncated standard normal, with support limited values inside the unit circle and Beta(1, 1) is the beta distribution with shape parameters of unity.

TABLE 4. Priors on initial conditions of the linear and nonlinear states.

Linear States	Nonlinear States
$\tau_0 \sim \mathcal{N}(2.0, 100.0^2)$	$\ln \varsigma^2_{\eta,0} \sim \ln\mathcal{N}(\ln 0.2 - 5.0, 10.0)$
$\mathbf{F}_0\tau_0 \sim \mathcal{N}(2.0, 100.0^2)$	$\ln \varsigma^2_{\nu,0} \sim \ln\mathcal{N}(\ln 0.4 - 5.0, 10.0)$
$\varepsilon_0 \sim \mathcal{N}(0.0, \sigma^2_{\varepsilon_0})$	$\theta_0 \sim \mathcal{TN}(0.0, 1.0; \theta_0 \in (-1, 1))$
$\mathbf{F}_0\varepsilon_0 \sim \mathcal{N}(0.0, \sigma^2_{\mathbf{F}_0\varepsilon_0})$	$\lambda_0 \sim \mathcal{TN}(0.5, 1.0; \lambda_0 \in (0, 1))$

Note: The priors on ε_0 and $\mathbf{F}_0\varepsilon_0$ are drawn jointly from $\mathcal{N}(\mathbf{0}_{2\times1}, \boldsymbol{\Sigma}^{(i)}_{\varepsilon,0})$, where $\sigma^2_{\varepsilon_0}$ and $\sigma^2_{\mathbf{F}_0\varepsilon_0}$ are the diagonal elements of

$$\boldsymbol{\Sigma}^{(i)}_{\varepsilon,0} = \sum_{j=0}^{\infty} \begin{bmatrix} \theta_0^{(i)} & 0 \\ (1-\lambda_0^{(i)})\theta_0^{(i)} & \lambda_0^{(i)}\theta_0^{(i)} \end{bmatrix}^j \begin{bmatrix} \varsigma^{2,(i)}_{\nu,0} & \lambda_0^{(i)}\varsigma^{2,(i)}_{\nu,0} \\ \lambda_0^{(i)}\varsigma^{2,(i)}_{\nu,0} & \lambda_0^{2,(i)}\varsigma^{2,(i)}_{\nu,0} \end{bmatrix} \begin{bmatrix} \theta_0^{(i)} & (1-\lambda_0^{(i)})\theta_0^{(i)} \\ 0 & \lambda_0^{(i)}\theta_0^{(i)} \end{bmatrix}^j,$$

and $\theta_0^{(i)}$, $\lambda_0^{(i)}$, and $\varsigma^{2,(i)}_{\nu,0}$ are the ith particle draws from priors on the associated initial conditions. For models where θ_t and λ_t, respectively, are static parameters, prior draws for these parameters appear in place of these initial values.

4.3 *The data*

The data are real-time realized inflation, π_t, and average SPF nowcast and 1-, 2-, 3-, and 4-quarter ahead forecasts. We obtain the data from the Real-Time Data Set for Macroeconomists (RTDSM) that is made available by the Federal Reserve Bank (FRB) of Philadelphia.

During each quarter t, the SPF collects inflation predictions from its respondents without full knowledge of π_t. At time t, the available real-time data for inflation typically reflects data releases that contain only observations through quarter $t-1$. We comply with this timing protocol by assuming that SPF forecasts collected in the middle of quarter t are formed conditional on information available at the end of quarter $t-1$, and denote the h step ahead SPF forecast collected at t by $\pi^{\text{SPF}}_{t-1,t+h}$. All told, our data set comprises readings on π_t and $\pi^{\text{SPF}}_{t,t+h}$ for $h = 1, 2, 3, 4, 5$.

The SPF provides forecasts for several inflation measures, including PCE and CPI data as well as the GNP/GDP deflator.[26] However, only for the latter, there is forecast data extending back to the Great Inflation years of the 1970s.[27] We use inflation predictions and realizations based on the GNP/GDP deflator from 1968Q4 to 2018Q3.[28]

[26]The SPF measured the price level of output with the implicit GNP deflator before 1992Q1. From 1992Q1 to 1996Q4, the implicit GDP deflator played this role. It was replaced by the chain weighted GDP deflator beginning in 1997Q1.

[27]The Online Supplementary Appendix provides complementary results obtained from CPI forecasts collected by the SPF since 1981. Similar to what is reported here, we find a significant up-tick in the stickiness parameter λ_t by the mid-1990s, when using a state space model where λ_t is time-varying. However, the shorter data does not allow anymore to conclusively distinguish between the different state space models listed in Table 1 above.

[28]There are missing observations for $\pi^{\text{SPF}}_{t,t+5}$ during 1969, 1970, and 1974, which are accommodated by modified observation equations in each model as needed.

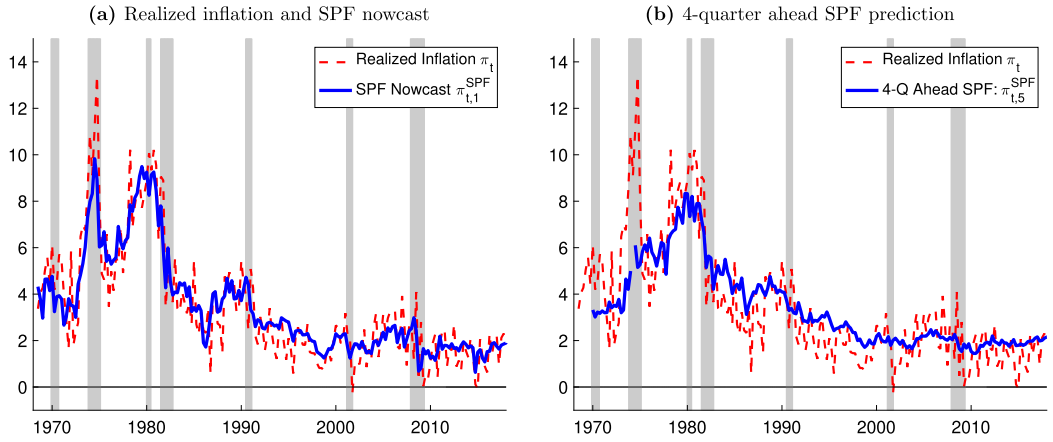

FIGURE 1. Realized inflation and SPF predictions. *Note*: Data from 1968Q4 to 2018Q3. Vertical gray bands denote NBER dated recessions.

Our measure of realized inflation is based on second-release data for the GNP/GDP deflator.[29] The RTDSM compiles the second-release data of the GNP/GDP deflator in growth rates. We convert the annualized growth rate, $G_t = 100((P_t/P_{t-1})^4 - 1)$, into continuously compounded growth rates using $\pi_t = \ln(1 + G_t/100)$. The SPF solicits forecasts for the GDP/GNP deflator in levels. We convert these price levels into expected growth rates by differencing the logs of the level forecasts.[30]

Figure 1 displays π_t and the average SPF predictions. The data has several interesting features. First, Figure 1 shows π_t is more volatile than the average SPF inflation predictions. Second, the average SPF inflation predictions are smoother and more centered on π_t as h increases. For example, Figure 1(a) shows the average SPF inflation nowcast, $\pi^{SPF}_{t,t+1}$, moving with π_t, during the inflation spikes of the 1973–1975 recession and the double dip recessions of the early 1980s. However, the spikes in the average SPF inflation predictions around these recessions are inversely related to h as illustrated in Figure 1(b) for the case of $h = 5$. Even after the Volcker disinflation, which had ended by 1986 according to Meltzer (2014, p. 1209), π_t continued to strongly fluctuate around $\pi^{SPF}_{t,t+5}$, though less persistently than before.

4.4 *Posterior estimates of the static parameters and model fit*

Table 5 lists moments of the posterior distributions for the parameters of our four state space models for the full data sample from 1968Q4 through 2018Q3. The reported moments are the posterior median and 90% uncertainty bands (i.e., 5 and 95% quantiles) that are displayed in brackets. Log MDDs are reported at the bottom of Table 5. Each state space model has been estimated with $M = 100{,}000$ particles.

[29]Second-release data for 1995Q3 are unavailable because of a federal government shutdown. We fill in the missing observations with the corresponding third-release data collected by the RTDSM.

[30]As is common in the literature evaluating SPF forecasts, the procedure constructing average inflation predictions from SPF price-level predictions ignores Jensen-inequality effects that result from the conversion of level forecasts into log differences; see, for example, Aruoba (2018).

TABLE 5. Parameter estimates and log MDDs of the state space models.

Parameter	Models			
	$\mathcal{M}_0$	$\mathcal{M}_1$	$\mathcal{M}_2$	$\mathcal{M}_3$
	Variances of shocks to SV processes			
σ_η^2 (Trend SV)	0.037	0.051	0.020	0.018
	[0.026, 0.048]	[0.036, 0.150]	[0.015, 0.028]	[0.013, 0.027]
σ_v^2 (Gap SV)	0.006	0.232	0.045	0.036
	[0.005, 0.009]	[0.026, 0.329]	[0.021, 0.074]	[0.026, 0.052]
	Persistence of inflation gap			
θ	0.758	0.707	–	–
	[0.663, 0.854]	[0.635, 0.780]		
σ_ϕ^2	–	–	0.001	0.003
			[0.001, 0.001]	[0.002, 0.004]
	Forecast stickiness			
λ	–	0.307	–	0.324
		[0.175, 0.373]		[0.268, 0.383]
σ_κ^2	0.005	–	0.008	–
	[0.004, 0.007]		[0.005, 0.010]	
	Measurement error variances			
$\sigma_{\zeta,\pi}^2$	0.517	0.778	0.612	0.486
	[0.429, 0.621]	[0.644, 0.939]	[0.519, 0.723]	[0.403, 0.592]
$\sigma_{\zeta,1}^2$	0.113	0.008	0.101	0.136
	[0.096, 0.135]	[0.007, 0.010]	[0.085, 0.122]	[0.116, 0.161]
$\sigma_{\zeta,2}^2$	0.042	0.008	0.042	0.042
	[0.035, 0.051]	[0.007, 0.010]	[0.036, 0.051]	[0.035, 0.051]
$\sigma_{\zeta,3}^2$	0.044	0.008	0.044	0.043
	[0.037, 0.052]	[0.007, 0.010]	[0.037, 0.053]	[0.036, 0.051]
$\sigma_{\zeta,4}^2$	0.047	0.008	0.044	0.050
	[0.040, 0.055]	[0.007, 0.010]	[0.037, 0.054]	[0.041, 0.060]
$\sigma_{\zeta,5}^2$	0.063	0.008	0.066	0.059
	[0.054, 0.075]	[0.007, 0.010]	[0.054, 0.079]	[0.049, 0.074]
$\ln \text{MDD}(\mathcal{M}_i \mid \mathcal{Y}^T)$	−528.964	−535.401	−520.613	−527.144
	(0.421)	(0.486)	(0.349)	(0.394)

Note: The table contains posterior moments and log MDDs for the state space models $\mathcal{M}_0$, $\mathcal{M}_1$, $\mathcal{M}_2$, and $\mathcal{M}_3$ based on $M = 100{,}000$ particles and the full data sample from 1968Q4 through 2018Q3. The main entry for every static parameter reports its posterior median with 5 and 95% quantiles in brackets below. Log MDDs for model i are denoted $\ln \text{MDD}(\mathcal{M}_i \mid \mathcal{Y}^T)$ and computed using equation (16). The reported values are the average estimates obtained from 250 repetitions of the particle learning filter, and the associated numerical standard errors appear in parentheses below each estimate.

Estimates of the static parameters differ in several ways. As shown in Table 5, estimates of σ_η^2 and σ_v^2, the variances of shocks to SV, are more diverse across the four state space models than estimates of the other static parameters. The shock variance of trend SV, σ_η^2, is estimated to be relatively small in the cases of $\mathcal{M}_2$ and $\mathcal{M}_3$, where gap persistence θ_t is time-varying. In contrast, $\mathcal{M}_1$, where both λ and θ are constant, is responsible

for relatively high posterior medians of σ_η^2 and σ_v^2, with corresponding estimates from $\mathcal{M}_0$ falling in between these cases. This suggests that SV in trend and gap inflation has to adjust more when gap persistence, $\theta_t = \theta$, and forecast stickiness, $\lambda_t = \lambda$ are held fixed. In particular, variations in trend SV seem to soak up changes in inflation dynamics otherwise captured by time-varying gap persistence.

In addition, the $\mathcal{M}_1$ case, when λ and θ are held fixed, produces the largest posterior median estimate for the variability of the irregular component of inflation, $\sigma_{\zeta,\pi}^2$, and the smallest posterior median estimates of measurement error variances in the survey equations, $\sigma_{\zeta,1}^2, \ldots, \sigma_{\zeta,5}^2$. The reason is a greater share of the variation in π_t is loaded onto the irregular component, while estimates of trend and persistent gap inflation are more closely aligned with SPF inflation predictions than current inflation. Otherwise, the static parameter estimates are broadly similar across models.

The log MDDs of $\mathcal{M}_0$, $\mathcal{M}_1$, $\mathcal{M}_2$, and $\mathcal{M}_3$, reported at the bottom of Table 5, are estimated using equation (16). We average over 250 repetitions of the particle learning filter to calculate the log MDDs. Uncertainty over the log MDDs resulting from the SMC approximation is measured using the numerical standard errors of the log MDD estimates computed on the 250 repetitions. Our use of numerical standard errors for gauging the uncertainty of simulation-based estimates is grounded in the work of Geweke (1989); see also Fuentes-Albero and Melosi (2013), and Herbst and Schorfheide (2014) for applications in the context of log MDD estimates. Table 5 shows that the difference between the log MDD associated with $\mathcal{M}_0$ and the other three alternatives is always greater than 6.5, which, in the language of Kass and Raftery (1995), constitutes very strong evidence in favor of $\mathcal{M}_2$. Moreover, the numerical standard errors of the log MDD estimates are thwarted by these differences in the log MDD. Hence, our discussion is centered on estimates produced using $\mathcal{M}_2$.[31]

Figure 2 plots particle learning filter estimates of the scale volatility parameters σ_η^2, σ_v^2, σ_ϕ^2, and σ_κ^2 of $\mathcal{M}_2$. Paths of these estimates appear in Figures 2(a), 2(b), 2(c), and 2(d) along with 68% and 90% uncertainty bands in dark and light shades. The plots show estimates of σ_η^2, σ_ϕ^2, and σ_κ^2 that cease to change much, if at all, after 1983. The exception is σ_v^2. In Figure 2(b), the static scale volatility of $\ln \varsigma_{v,t}^2$ in $\mathcal{M}_2$ drifts up during the sample and especially after 1983. Between 1983 and the end of the sample, σ_v^2 almost doubles in size from about 0.025 in 1983$Q1$ to 0.045 at 2018$Q3$ while its 90% uncertainty bands are widest running from 0.02 to 0.15 after the 2007–2009 recession.

4.5 *Trend and gap inflation*

Estimates of trend and gap inflation produced by $\mathcal{M}_2$ are shown in Figure 3. Figure 3(a) compares realized inflation, π_t, the 4-quarter ahead average SPF inflation prediction, $\pi_{t,t+5}^{\text{SPF}}$, and filtered estimates of RE trend inflation, $\tau_{t|t}$.

Figure 3(a) gives evidence of the role $\pi_{t,t+5}^{\text{SPF}}$ has in estimating trend inflation. Before the Volcker disinflation, $\pi_{t,t+1}^{\text{SPF}}$ often deviates substantially from $\tau_{t|t}$. This relationship is

[31] Estimates of $\mathcal{M}_0$, $\mathcal{M}_1$, and $\mathcal{M}_3$ are in the Online Supplementary Appendix. There, we also present broadly similar estimates from model specifications that omit the irregular component, $\zeta_{\pi,t}$, from the process for π_t. However, these specifications are not favored by the data in terms of log MDDs.

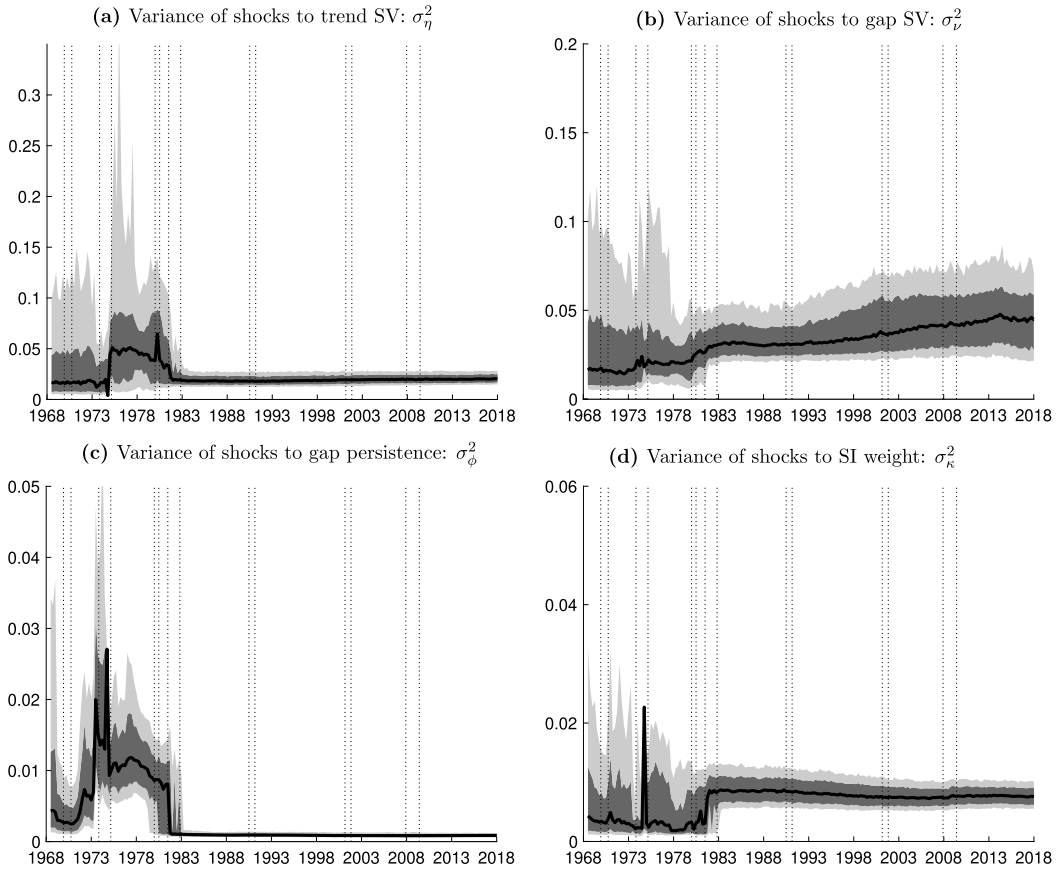

FIGURE 2. Particle learning filter estimates of static parameters. *Note*: Posterior quantiles of particle-learning paths of several static parameters of the state space model $\mathcal{M}_2$ based on data from 1968Q4 through 2018Q3. In each panel, the solid line depicts the posterior median while the dark and light shaded areas correspond to 68% and 90% uncertainty bands, respectively. Dotted vertical lines denote NBER recession peaks and troughs.

reversed mostly from the end of the Volcker disinflation to 2018Q3. The spread between $\pi_{t,t+5}^{\text{SPF}}$ and $\tau_{t|t}$ is smaller during the 1973–1975 recession, the double-dip recessions of the early 1980s, and the Volcker disinflation. From 1990 to the end of the sample, $\pi_{t,t+5}^{\text{SPF}}$ fluctuates around $\tau_{t|t}$. This suggests that estimates of trend inflation rely on the 4-quarter ahead average SPF inflation prediction.

Mechanically, our model's measurement equations (13) link longer-horizon SI forecasts closely to the SI trend.[32] In addition, our model implies a close link between SI and RE trend, with their difference evolving as a stable AR(1) process, whose persistence and innovation variance scales with the sticky-information weight:

$$(\mathbf{F}_t\tau_t - \tau_t) = \lambda_t(\mathbf{F}_{t-1}\tau_{t-1} - \tau_{t-1}) - \lambda_t\sigma_{\eta,t}\eta_{t-1}.$$

[32]As noted by Kozicki and Tinsley (2012) in the context of modeling RE forecasts, for $h \to \infty$, the UC model equates survey predictions with the SI trend plus measurement error.

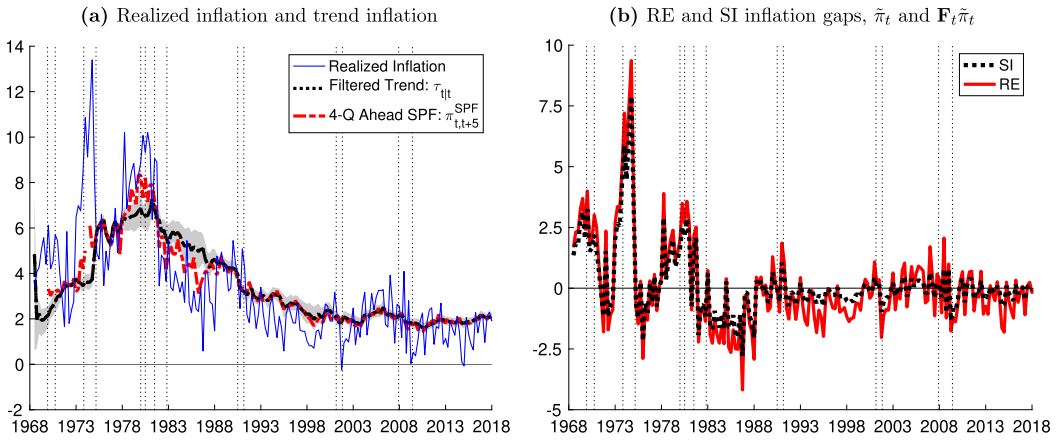

FIGURE 3. Estimates of trend and gap inflation. *Note*: Filtered estimates obtained from model $\mathcal{M}_2$ using data from 1968Q4 to 2018Q3. Light gray shaded areas in panel (a) represent 68% uncertain bands around estimates of filtered RE trend inflation, $\tau_{t|t}$. Panel (b) depicts filtered estimates of RE and SI gap inflation, $\tilde{\pi}_{t|t}$ and $F_{t|t}\tilde{\pi}_t$. In both panels, vertical dotted bands denote NBER dated recessions.

Evidently, when stickiness, λ_t, is low, differences between SI and RE trend are small and not persistent. Moreover, the smaller trend SV, $\sigma_{\eta,t}$, the smaller the differences between RE and SI trend. Strikingly, estimates of SI trend inflation, $\mathbf{F}_{t|t}\tau_t$, reported in the Online Supplementary Appendix, are nearly identical to the RE trend, $\tau_{t|t}$, throughout the entire sample. Estimates of λ_t and $\sigma_{\eta,t}$, presented further below, account for the closeness between SI and RE trend with low stickiness during the first-half of the sample, and low trend SV during the second-half of the sample.

Not surprisingly, realized inflation displays more variability than trend inflation in Figure 3(a). During the first oil price shock, π_t is a third or more greater than $\tau_{t|t}$. However, trend inflation explains much of the persistent increases in π_t during the late 1970s and early 1980s. With the onset of the Volcker disinflation, π_t tracks persistently below trend inflation until the late 1990s, and then again after the Great Recession of 2007–2009.

Figure 3(b) displays estimates of RE and SI versions of the inflation gap, $\tilde{\pi}_t$ in (2), which is the sum of the persistent and noisy gap components. Both gap measures rise from about -2% in 1968Q4 to almost 4% in 1970. The 1973–1975 recession sees the largest spikes in gap inflation reaching 9% or more before falling to about -2.5% by 1976. Between the Volcker disinflation and the end of the 1980s, gap inflation is negative and mostly below -2.0%.

During the 1970s and 1980s, RE and SI inflation gaps track each other quite closely. Starting with the 1990s, however, both measures begin to markedly differ. SI gap inflation becomes noticeably smoother than its RE counterpart, and hovers mostly near zero. In contrast, RE gap inflation is more volatile but without much persistence. Toward the end of the Great Recession in 2009, both gap measures move again more in tandem as they drop persistently for a few quarters.

Our estimates of the linear states are a counterpoint to studies that find either trend or gap inflation to dominate movements in realized inflation. Stock and Watson (2007) presented estimates of trend inflation that largely track realized inflation while Cogley and Sbordone (2008) reported estimates of trend inflation that are smooth and point to the dominance of gap inflation in explaining realized inflation. Figure 3 shows that conditioning estimates of $\mathcal{M}_2$ on average SPF inflation predictions produces estimates of trend and gap inflation that fall somewhere between these polar cases. For example, most of the inflation spike around the 1973–1975 recession is attributed to gap inflation by $\mathcal{M}_2$. However, by the late 1970s and 1980 recession, trend inflation accounts for a larger share of the surge in realized inflation.

We attribute these differences with other studies mainly to two factors: First, persistence in gap inflation allows the model to identify persistent, but nonpermanent changes in inflation as gap rather than trend inflation. Second, the assumed cointegration between realized inflation and the observed term-structure of SPF forecasts provides a clearer signal about trend inflation.

We can also infer the beliefs the average SPF respondent has about the future path of realized inflation. For example, SI gap inflation is negative for most of the 1980s, while trend inflation remained fairly elevated. These estimates suggest the average SPF participant anticipated the Volcker disinflation would only produce a transitory drop in realized inflation, which is consistent with Goodfriend and King (2005) and Meltzer (2014, p. 1131). They argue households, firms, and investors expected the Volcker disinflation would only produce a transitory decline in inflation after 1984. Similarly, trend inflation is fairly unchanged after 2007, and mostly above π_t, indicating the average member of the SPF expected realized inflation to eventually rise back to the pre-crisis trend.

4.6 *Stochastic volatility in trend and gap inflation*

The state space model $\mathcal{M}_2$ yields estimates of filtered stochastic volatilities, $\varsigma_{\eta,t|t}$ and $\varsigma_{v,t|t}$, that appear in Figure 4; smoothed estimates are presented in the Online Supplentary Appendix. Overall, estimated volatilities of trend shocks, $\varsigma_{\eta,t|t}$ are often smaller than their counterparts for gap shocks, $\varsigma_{v,t|t}$. The largest peaks in $\varsigma_{\eta,t|t}$ occur in 1978 and 1980, as shown on Figure 4(a) while $\varsigma_{v,t|t}$ is dominated by spikes in 1975–1976 and 1978 shown in Figure 4(b). Another revealing feature of these figures is that $\varsigma_{\eta,t|t}$ and $\varsigma_{v,t|t}$ often rise during or after a NBER recessions.

Our estimates of trend and gap inflation stochastic volatilities differ somewhat from Grassi and Proietti (2010), Stock and Watson (2007, 2016), among others. These authors report trend stochastic volatility dominates inflation gap stochastic volatility from the 1970s well into the late 1990s. In contrast, Figure 4 attributes the jumps in inflation volatility during the 1970s, 1980s, and 1990 in good part to increases in the volatility of transitory shocks rather than mostly reflecting volatility in trend inflation. This suggests that our approach to estimating the inflation gap persistence parameter has a substantial impact on estimates of the trend volatilities affecting the innovations to trend and gap inflation.

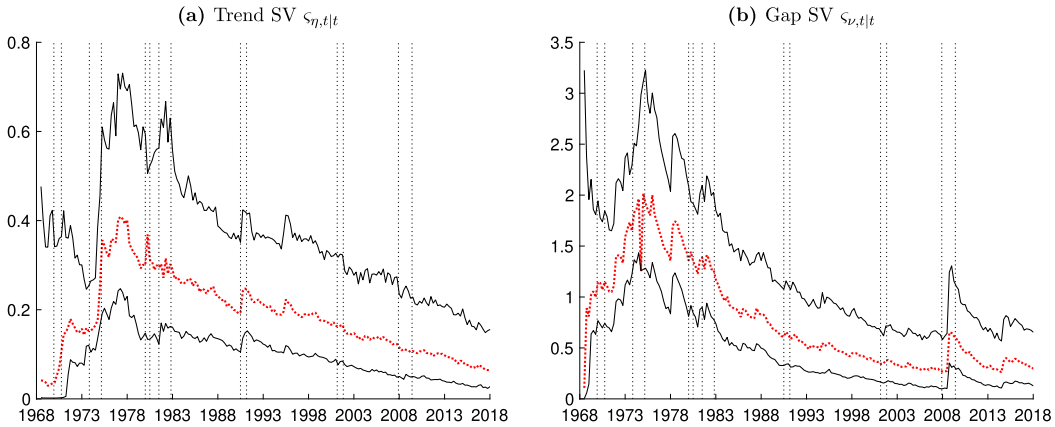

FIGURE 4. Stochastic volatility in trend and gap inflation. *Note*: Filtered estimates obtained from model $\mathcal{M}_2$ using data from 1968Q4 to 2018Q3. Dotted lines represent medians, solid thin lines are lower and upper bounds on 90% uncertainty bands. Vertical dotted bands denote NBER dated recessions.

4.7 *Drifting inflation gap persistence and sticky-information updating*

This section presents evidence to illustrate why the data prefers $\mathcal{M}_2$. By comparing estimates of θ_t and λ_t to estimates of θ and λ gleaned from $\mathcal{M}_1$ and $\mathcal{M}_0$, we argue countercyclical movements of the drifting persistence parameter of the inflation gap before the Volcker disinflation combined with upward drift in the sticky-information weight post-1990 explains why the data favors $\mathcal{M}_2$ over the other state space models.

Figures 5(a) and 5(b) begins the discussion with two different kinds of estimates of the inflation gap persistence parameter and sticky-information weight. These figures contain dot–dash lines that are filtered estimates of the drifting inflation gap persistence parameter and sticky-information weight, $\theta_{t|t}$ and $\lambda_{t|t}$, of $\mathcal{M}_2$. Applying our particle learning filter to $\mathcal{M}_1$ produces paths of θ and λ that are the solid lines in Figures 5(a) and 5(b). The paths of θ and λ are surrounded by 90% uncertainty bands denoted by thin dot–dash lines while the light gray shading represent 90% uncertainty bands of $\theta_{t|t}$ and $\lambda_{t|t}$.

The estimates of $\mathcal{M}_1$ indicate the path of θ shifts from countercyclical to acyclical comovement with the NBER dated recessions by the early 1980s. Figure 5(a) depicts the path of θ peaking at more than 0.8 during the 1969–1970 and 1973–1975 recessions while dropping almost to zero in 1972 and early 1973. From 1976 to the end of the sample, this path often wobbles, but is never less than 0.6 or greater than 0.8. The 90% uncertainty bands for the path of θ are narrow for most of the sample.

Figure 5(a) also shows that by 1980 $\theta_{t|t}$ experiences a similar change in its comovement with the business cycle. During the 1969–1970 and 1973–1975 recessions, $\theta_{t|t}$ peaks. In the expansions that follow these recessions, there are troughs in $\theta_{t|t}$ that are near zero in 1972 and 1977. There is a third peak in $\theta_{t|t}$ that almost reaches one (its upper bound) in 1979. Subsequently, $\theta_{t|t}$ falls to near 0.7 at the start of the 1981–1982 recession and fluctuates between 0.65 and 0.85 for the rest of the sample. Hence, $\theta_{t|t}$ is counter-

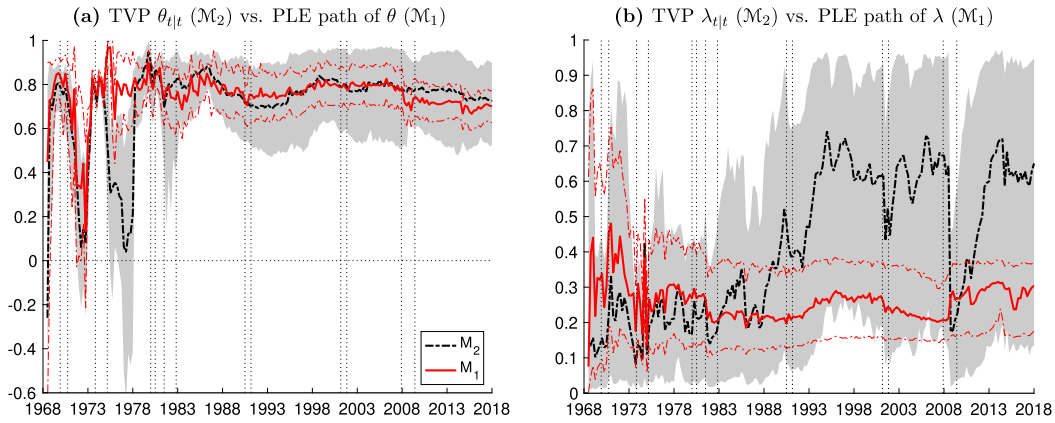

FIGURE 5. Gap persistence and sticky-information weight under $\mathcal{M}_1$ vs. $\mathcal{M}_2$. *Note*: Comparison of estimates obtained from models $\mathcal{M}_1$ (PLE paths of static parameters) and $\mathcal{M}_2$ (filtered estimates of time-varying parameters) based on data from 1968Q4 to 2018Q3. The light gray shaded areas and dash–dotted lines areas depict 90% uncertainty bands around median estimates of static and drifting parameter versions of θ and λ produced by the two models. The vertical dotted bands denote NBER dated recessions.

cyclical pre-1980 and acyclical post-1980. The sampling uncertainty surrounding $\theta_{t|t}$ is widest after the 1973–1975 recession and during the 1981–1982 recession.

The shift in the behavior of inflation gap persistence over the business cycle is consistent with Meltzer (2014, p. 1006 and p. 1207). He contends that Fed monetary policy became more concerned with inflation control since the Volcker disinflation, thus causing less persistent swings in inflation than during the 1970s. Our estimates of the inflation gap persistence parameter in $\mathcal{M}_1$ and $\mathcal{M}_2$ indicates the average member of the SPF agrees with Meltzer.

The sticky-information weights produced by estimating $\mathcal{M}_2$ and $\mathcal{M}_1$ are found in Figure 5(b). These estimates show the paths of $\lambda_{t|t}$ and λ deviate after 1988. During the first half of the sample, λ and $\lambda_{t|t}$ are close and always less than a half. The path of λ continues to show that sticky-information forecast were updated quite frequently until the end of the sample. Strikingly, $\lambda_{t|t}$ begins to increase after 1988. By 1995, the frequency of sticky-information inflation forecast updating is about three quarters on average. This holds for the rest of the sample with one exception. Between 2009 and 2014, $\lambda_{t|t}$ follows a V-shaped path. The frequency of sticky-information inflation forecast updating approximates rational expectations in 2009, but bounces back to the pre-recession frequency of sticky-information inflation forecast updating by 2014.

Filtered estimates of the drifting inflation gap persistence parameter and sticky-information weight provide evidence for the preference of the data for $\mathcal{M}_2$. Figure 5 presents two kinds of evidence. One piece of evidence is the countercyclical behavior of $\theta_{t|t}$ pre-Volcker disinflation and not after in Figure 5(a). Next, the drop in the frequency of sticky-information inflation forecast updating occurs about the same time estimates of rational-expectations and sticky-information trend inflation shown in Figure 3(c) and of filtered and smoothed stochastic volatilities plotted in Figure 4 also are falling.

Figure 5(b) displays 90% uncertainty bands of $\lambda_{t|t}$ that are almost always wider than the 90% uncertainty bands of the path of λ. The sampling uncertainty around $\lambda_{t|t}$ maps into an average frequency of sticky-information inflation forecast updating that runs from one to 10 quarters on average after 1990. The exception is the 2007–2009 recession when the 90% uncertainty bands of $\lambda_{t|t}$ narrow to between near zero and 0.4. However, as argued below, the width of these bands hides significant changes in λ_t over time.

Figure 6 reports filtered and smoothed estimates of the drifting sticky-information weight, λ_t, extracted from $\mathcal{M}_2$. Over the first-half of the sample, estimates of λ_t are fairly low and remain below 0.5 until the late 1980s. With the end of the Volcker disinflation, estimates of λ_t begin to rise markedly and move mostly around 0.6, except for a brief drop in the recession of 2008. The 90% uncertainty bands of $\lambda_{t|t}$ and $\lambda_{t|T}$ shown in Figure 6(a) are very wide except for several NBER dated recessions. However, as argued next, these bands reflect mostly uncertainty about the location, not the contours, of the estimated trajectories for λ_t.

To better assess the significance of changes in λ_t since the beginning of the sample, Figure 6(b) plots accumulated changes, $\lambda_{t|T} - \lambda_{1|T}$, with dark and light gray areas representing 68% and 90% uncertainty bands.[33] The figure shows 68% and 90% uncertainty bands of $\lambda_{t|T} - \lambda_{t|T}$ that are tight compared with the uncertainty bands of $\lambda_{t|T}$ in Figure 6(a). Strikingly, only from the 1973–1975 recession to about 1986 do these uncertainty bands cover zero except.

Estimates of the accumulated changes in the frequency of sticky-information inflation forecast updating, shown in Figure 6(b), are near zero from 1973 to 1988, but begin

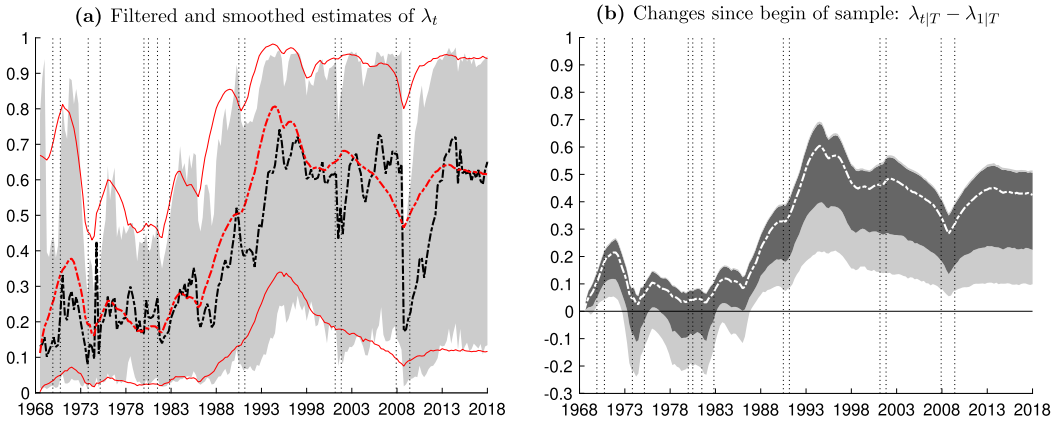

FIGURE 6. Time-variation in the sticky-information weight. *Note*: Estimates obtained from model $\mathcal{M}_2$ based on data from 1968Q4 to 2018Q3. Panel (a) displays filtered and smoothed estimates, surrounded by 90% bands. Panel (b) displays the change in smoothed estimates of the SI weight since the start of the sample, $\lambda_{t|T} - \lambda_{1|T}$, surrounded by 68% (dark gray) and 90% (light gray) uncertainty bands. Vertical dotted bands denote NBER dated recessions.

[33]Smoothed estimates, $\lambda_{t|T}$, reflect the same conditioning set irregardless of t. The changes in λ_t are thus computed only based on smoothed estimates, since those provide us with joint uncertainty bands for $\lambda_{t|T}$ and $\lambda_{1|T}$ that allow for proper measurement of the uncertainty around their difference.

to increase significantly in the early 1990s and reach a plateau by 1995. This plateau is roughly maintained until $\lambda_{t|T} - \lambda_{1|T}$ takes a V-shaped plunge during the 2007–2009 recession that is followed by a snap back to pre-recession levels by 2014. In Section 5, we juxtapose these estimates of upward drift in the SI weight after the Volcker disinflation, with estimates of a concurrent decline in inflation persistence.

Our estimates of an upward drift in survey forecast stickiness coincides with an increased anchoring of inflation expectations.[34] Notably, the rise in forecast stickiness peaks in the mid 1990s, around the time the Fed started to engage in a policy of "opportunistic disinflation," according to Meyer (1996) and Orphanides and Wilcox (2002). More broadly, the stickiness of inflation forecasts seems to have been unaffected by the episodes of "considerable" and "extended" policies, of the Greenspan and Bernanke Feds, and the host of unconventional post-2007 policies employed by the Bernanke and Yellen Feds. Interest rates are needed to evaluate the impact of monetary policy on inflation dynamics as studied, for example, by Leeper and Zha (2003). However, a possible speculation is that the extent to which these policies served to keep inflation expectations anchored also mitigated any incentive of survey expectations to become less sticky during these otherwise eventful episodes.

5. Uncertainty, persistence, and forecast stickiness

Up to this point, we have documented significant time-variation in forecast stickiness, as measured by the frequency of sticky-information forecast updating, λ_t. Among others, we find a noticeable drop in forecast stickiness around the 2007–2009 recession. Coibion and Gorodnichenko (2015) report broadly similar evidence of time variation in λ_t and point to recessions and the decline in macroeconomic volatility since the mid 1980s, also known as the Great Moderation, as proximate causes of forecast stickiness. This section complements their analysis by juxtaposing our estimates of λ_t with characteristics of the inflation process implied by our state space models.

We focus on two metrics characterizing the inflation process that should matter for forecasters. One metric is the mean squared error of the forecast (MSE). The second is the share of forecast error variance (FEV) attributable to nonpersistent shocks. We argue this forecast-error-variance share is a suitable proxy for inflation persistence. The estimates of stickiness, the MSE, and the variance share of nonpersistent shocks shown below are constructed from the posterior distribution of $\mathcal{M}_2$. The priors of $\mathcal{M}_2$ view time-variation in stickiness as unrelated to the underlying dynamics of inflation. Recall that, for parsimony and not to impose a specific form of state dependence on inflation forecast stickiness, we assume λ_t is driven by an exogenous shock. Nevertheless, as documented below, there is a striking resemblance between time-variation in estimates of inflation stickiness and the importance of persistent shocks in accounting for the MSE of inflation.

[34] Anchored inflation expectations imply a relatively low variability of long-run forecasts; by this metric, U.S. inflation became (re)anchored since the late 1980s as noted noted by Bernanke (2007), Stock and Watson (2007), Mertens (2016), Nason and Smith (forthcoming) and others.

Coibion and Gorodnichenko (2015) used the MSE of the sticky-information forecaster's h-step ahead prediction at a given date t as the dependent variable in their regression analysis to evaluate forecast stickiness.[35] The MSE of a sticky-information forecast, denoted SI-MSE, can be decomposed into the sum of squared bias and forecast error variance

$$\textbf{SI-MSE}_{t,h} \equiv \mathbf{E}_t\left\{(\pi_{t+h} - \mathbf{F}_t\pi_{t+h})^2\right\} = (\mathbf{E}_t\pi_{t+h} - \mathbf{F}_t\pi_{t+h})^2 + \textbf{Var}_t\pi_{t+h}. \tag{17}$$

The decomposition of equation (17) is the source of what is shown in Figure 7(a). The figure depicts time variation in the SI-MSE defined in equation (17) for $h = 1$ and the contributions from squared bias and forecast error variance over time.

We produce the results shown in Figure 7 from smoothed estimates of $\mathcal{M}_2$ to compute rational expectations and sticky-information forecasts as well the MSEs. This conditioning implies our estimates of MSE correspond to $\mathbf{E}\{\mathbf{E}_t(\pi_{t+h} - \mathbf{F}_t\pi_{t+h})^2|\mathcal{Y}^T\}$ rather than $\mathbf{E}\{(\pi_{t+h} - \mathbf{F}_t\pi_{t+h})^2|\mathcal{Y}^T\}$. The conditional moments $\mathbf{E}_t\{\cdot\}$ and $\textbf{Var}_t(\cdot)$ are evaluated from the perspective of a forecaster who knows the current level of inflation, its decomposition into trend, and persistent and irregular gap components, the stochastic volatilities, and static parameters. This approach is intended to capture the potentially richer information set of SPF respondents, relative to the econometrician, that drives forecast updating. (See the Online Supplementary Material for computational details.)

Figure 7(a) displays sizable variation in the SI-MSE over the entire sample. In line with Stock and Watson (2007) and Clark, McCracken, and Mertens (2019), uncertainty around inflation forecasts is greatest during the 1970s. The SI-MSE peaks around the 1973–1975 recession and remains elevated for the remainder of the 1970s. From the onset of the Volcker disinflation, forecast uncertainty, as measured by the SI-MSE, is mostly declining until the end of the sample. We obtain similar results for longer forecast horizons.

Considering the relative contributions of bias and forecast error variance, the SI-MSE is dominated by forecast error variance with squared bias playing only a minor role. Strikingly, extended periods of large biases (in absolute value) are rare throughout the sample. Moreover, squared bias becomes negligible since the late 1990s, which is when our filtered and smoothed estimates of λ_t increase to 0.6 or more. This evidence is consistent with the notion that the frequency of sticky-information inflation forecast updating may not have risen by accident, but rather reflects an evaluation of costs and benefits of forecast updating, as suggested, for example, by the theories and models of Sims (2003) and Mackowiak and Wiederholt (2009).

To support the hypothesis that variations in forecast stickiness may be related to changes in the inflation process, we consider a counterfactual experiment that takes as given our estimates of trend and gap components of the inflation process. We construct hypothetical SI forecasts of inflation that are based on the SI law of motion (7), but fix λ to a moderately high value of 0.6, roughly in line with our estimates of λ_t for the second-half of the sample.

[35] Absent a specific model of the sticky-information forecaster's loss function, squared errors are only a proxy for actual losses. Squared errors are a natural starting point for assessing the forecast errors of a sticky-information forecaster, since they are minimized by the rational-expectations benchmark.

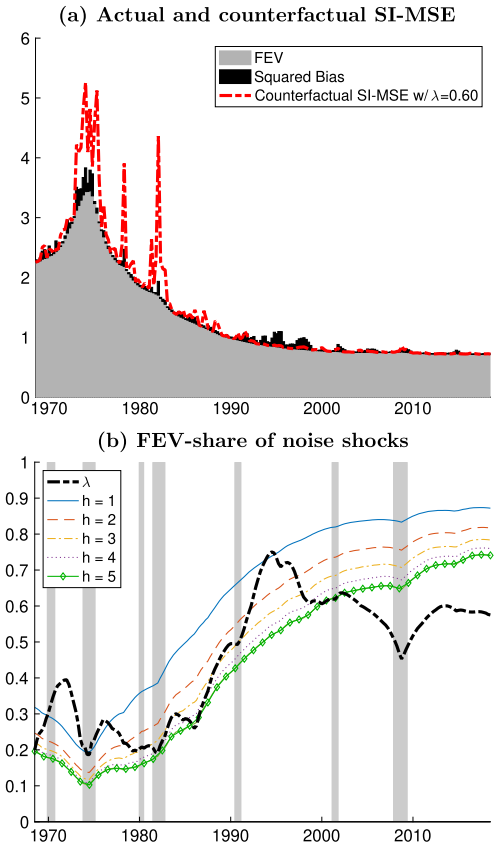

FIGURE 7. Forecast stickiness and the contribution of persistent shocks to inflation. *Note*: Panel (a) depicts the SI-MSE and its two components, forecast-error variance (FEV), and squared bias, as defined in equation (17) for $h = 1$. In addition, the panel also displays a counterfactual sticky-information MSE obtained from a sequence of SI forecasts constructed using $\lambda = 0.6$. Panel (b) compares the forecast error variance share of inflation at different horizons due to noise, as defined in (18), against smoothed estimates of the sticky-information weight, $\lambda_{t|T}$, of $\mathcal{M}_2$. Vertical dotted bands denote NBER dated recessions.

The resulting counterfactual SI-MSE for one-step ahead SI forecasts is shown in Figure 7(a).[36] The upshot is that if inflation forecast stickiness had been that high during the late 1970s, forecast bias would have been substantially higher than it actually was. This bias would have been about as high as the forecast-error variance associated with the optimal rational-expectations inflation forecast displayed in the same figure. This stands in contrast to the actual and counterfactual bias during the second-half of the sample, which are fairly small, even though both reflect elevated levels of inflation forecast stickiness. All told, the estimated increase in forecast stickiness occurs at a time when a lower frequency of SI forecast updating produces little difference between SI and

[36]By construction, actual and counterfactual SI-MSE differ only in their squared-bias components, and the implied counterfactual squared bias can be read off the figure as the difference between the forecast error variance and the counterfactual SI-MSE.

RE inflation forecasts. We document the relatively benign consequences of stickiness for forecast performance further in the Online Supplementary Appendix.

A key concern for forecasting is the importance of persistent shocks in the inflation process. In our state space models, inflation is the sum of three components: trend, and persistent, and irregular gaps. As described in Section 2, optimal rational-expectations inflation forecasts are linear combinations of the trend, τ_t, and the persistent gap component, ε_t, since the irregular gap component is serially uncorrelated noise. Greater volatility in the shocks to τ_t and ε_t increases the variability of optimal RE forecasts. Stochastic volatility causes the share of forecast error variance explained by each shock to vary over time. We contend that when shocks to τ_t and ε_t account for a larger share of variations in π_t a sticky-information forecaster has a greater incentive to update more frequently. As a result, forecast stickiness should be positively related to the share of forecast error variance due to the serially uncorrelated irregular component. For an h-step ahead forecast, this variance share is given by

$$\textbf{FEV-share-noise}_{t,h} = \frac{\sigma^2_{\zeta,\pi}}{\textbf{Var}_t \pi_{t+h}} = \frac{\sigma^2_{\zeta,\pi}}{\textbf{Var}_t \tau_{t+h} + \textbf{Var}_t \varepsilon_{t+h} + \sigma^2_{\zeta,\pi}}. \tag{18}$$

Indeed, as Figure 7(b) shows, the shares of h-step ahead forecast error variances due to the noise component mirrors variations in our smoothed estimates of the sticky-information weight, $\lambda_{t|T}$, for $h = 1, 2, \ldots, 5$.[37] While $\lambda_{t|T}$ suggests low levels of sticky information during the latter half of the 1970s and the Volcker disinflation, the stickiness of inflation forecast updating has risen since 1990 and remained high except for a brief dip during the 2007–2009 recession. During the first half of the sample, the share of forecast error variance due to the noise component in inflation was relatively low. As shown in Figure 7(b), this share increases at the same time as the Volcker disinflation takes hold and remains high for most of the remaining sample. The exception is a brief drop in the noise share during the 2007–2009 recession, that is also mirrored by an even more pronounced dip in $\lambda_{t|T}$. In contrast, total forecast uncertainty (measured by FEV) has been declining steadily since the 1970s with only a minimal increase during the 2007–2009 recession, as seen in Figure 7(a).

In sum, we obtain substantial evidence of an increase in the stickiness of SPF inflation predictions that lines up with a decline in inflation persistence after the Volcker disinflation. Our model is not structural; nevertheless, the evidence suggests that forecast stickiness may not be invariant to the inflation process and the monetary policy framework shaping it.

6. Conclusions

This paper studies the joint dynamics of realized inflation and the term structure of average inflation predictions in the Survey of Professional Forecasters (SPF). We build nonlinear state space models using the Stock and Watson unobserved components model

[37] In the Online Supplementary Appendix, we report similar results based on an alternative decomposition of the forecast error variances. Based on a metric used by Cogley, Primiceri, and Sargent (2010), this alternative persistence measure reflects the relative variability of h-step ahead inflation expectations.

and the Coibion and Gorodnichenko (2015) version of the Mankiw and Reis (2002) sticky-information model to estimate trend and gap inflation, the stochastic volatility affecting these states, the inflation gap persistence parameter, and the sticky-information weight. The state space models are estimated on a sample of realized inflation and averages of SPF inflation predictions from 1968$Q4$ to 2018$Q3$ using sequential Monte Carlo methods. The sequential Monte Carlo methods consist of a particle learning filter proposed by Carvalho et al. (2010) and a Rao–Blackwellized particle smoother developed by Lindsten et al. (2016).

We draw four headline results from our estimates: First, the 4-quarter ahead average SPF inflation prediction has information that increases the efficiency of estimates of trend inflation. Second, inflation gap persistence flips from countercyclical before the Volcker disinflation to acyclical for the remainder of the sample. Third, the stickiness of inflation forecasts increases after the Volcker disinflation. This remains the case to the end of the sample except for a transitory decline in the sticky-information weight during the 2007–2009 recession. Fourth, shifts in the stickiness of inflation forecasts occur at the same time the importance of persistent shocks for explaining the variation in realized inflation begins to decline. This evidence suggests that sticky-information inflation forecasts are state dependent, but without business-cycle dependence. The lesson for central banks is to engage in policies that prevent private agents from anticipating that persistent shocks will dominate movements in inflation.

Our results fit into a literature that finds permanent shocks matter more to professional forecasters than transitory shocks. In particular, we find changes in the frequency of forecast updating that coincide with a decline in the importance of persistent shocks for inflation dynamics. In our view, this evidence should point future research toward endogenizing the sticky-information weight, perhaps, in the tradition of rational inattention models of Sims (2003) and Mackowiak and Wiederholt (2009). We hope our paper stimulates further work on the ways in which professional forecasters and other economic agents process information to form beliefs and predictions about future economic outcomes and events.

References

Andrieu, C., A. Doucet, and R. Holenstein (2010), "Particle Markov chain Monte Carlo methods." *Journal of the Royal Statistical Society, Series B*, 72 (3), 269–342. [1493]

Ang, A., G. Bekaert, and M. Wei (2007), "Do macro variables, asset markets, or surveys forecast inflation better?" *Journal of Monetary Economics*, 54 (4), 1163–1212. [1486]

Aruoba, S. B. (2018), "Term structures of inflation expectations and real interest rates." *Journal of Business & Economic Statistics*, 38, 542–553. [1503]

Ascari, G., P. Bonomolo, and H. F. Lopes (2019), "Walk on the wild side: Temporarily unstable paths and multiplicative sunspots." *American Economic Review*, 109 (5), 1805–1842. [1488]

Atkeson, A. and L. E. Ohanian (2001), "Are Phillips curves useful for forecasting inflation?" *Quarterly Review, Federal Reserve Bank of Minneapolis*, 25, 2–11. [1486]

Bernanke, B. S. (2007), "Inflation expectations and inflation forecasting." Remarks given at the *Monetary Economics Workshop of the National Bureau of Economic Research Summer Institute*, Cambridge, MA (July 10). [1486, 1512]

Beveridge, S. and C. R. Nelson (1981), "A new approach to decomposition of economic time series into permanent and transitory components with particular attention to measurement of the business cycle." *Journal of Monetary Economics*, 7 (2), 151–174. [1489]

Carvalho, C. M., M. S. Johannes, H. F. Lopes, and N. G. Polson (2010), "Particle learning and smoothing." *Statistical Science*, 25 (1), 88–106. [1488, 1493, 1494, 1496, 1498, 1516]

Chen, R. and J. S. Liu (2000), "Mixture Kalman filters." *Journal of the Royal Statistical Society, Series B*, 62 (3), 493–508. [1495]

Clark, T. E., M. W. McCracken, and E. Mertens (2019), "Modeling time-varying uncertainty of multiple-horizon forecast errors." *Review of Economics and Statistics*, 102, 17–33. [1513]

Cogley, T., G. Primiceri, and T. J. Sargent (2010), "Inflation-gap persistence in the US." *American Economic Journal: Macroeconomics*, 2 (1), 43–69. [1487, 1515]

Cogley, T. and T. J. Sargent (2015), "Measuring price-level uncertainty and instability in the U.S., 1850–2012." *Review of Economics and Statistics*, 97 (4), 827–838. [1489]

Cogley, T. and A. Sbordone (2008), "Trend inflation, indexation, and inflation persistence in the new Keynesian Phillips curve inflation-gap persistence in the US." *American Economic Review*, 98 (5), 2101–2126. [1508]

Coibion, O. and Y. Gorodnichenko (2012), "What can survey forecasts tell us about informational rigidities?" *Journal of Political Economy*, 120 (1), 116–159. [1486]

Coibion, O. and Y. Gorodnichenko (2015), "Information rigidity and the expectations formation process: A simple framework and new facts." *American Economic Review*, 105 (8), 2644–2678. [1486, 1490, 1512, 1513, 1516]

Creal, D. (2012), "A survey of sequential Monte Carlo methods for economics and finance." *Econometric Reviews*, 31, 245–296. [1488, 1489]

Croushore, D. (2010), "An evaluation of inflation forecasts from surveys using real-time data." *The B.E. Journal of Macroeconomics*, 10 (1), 1–32. [1487]

Djuric, P. and J. Miguez (2002), "Sequential particle filtering in the presence of additive Gaussian noise with unknown parameters." In *IEEE International Conference on Acoustics, Speech, and Signal Processing*, Vol. 2, 1621–1624. [1497]

Faust, J. and J. H. Wright (2013), "Forecasting inflation." In *Handbook of Economic Forecasting*, Vol. 2 (G. Elliot and A. Timmermann, eds.), Chapter 1, 2–56, Elsevier, Amsterdam. [1486, 1490]

Fearnhead, P. (2002), "Markov chain Monte Carlo, sufficient statistics, and particle filters." *Journal of Computational and Graphical Statistics*, 11 (4), 848–862. [1497]

Fuentes-Albero, C. and L. Melosi (2013), "Methods for computing marginal data densities from the Gibbs output." *Journal of Econometrics*, 175 (2), 132–141. [1505]

Geweke, J. (1989), "Bayesian inference in econometric models using Monte Carlo integration." *Econometrica*, 57 (6), 1317–1339. [1505]

Godsill, S. J., A. Doucet, and M. West (2004), "Monte Carlo smoothing for nonlinear time series." *Journal of the American Statistical Association*, 99, 156–168. [1498]

Goodfriend, M. and R. G. King (2005), "The incredible Volcker disinflation." *Journal of Monetary Economics*, 52 (5), 981–1015. [1487, 1508]

Gordon, N., D. Salmond, and A. F. M. Smith (1993), "Novel approach to nonlinear/non-Gaussian Bayesian state estimation." *IEE Proceedings F, Radar Signal Processing*, 140 (2), 107–113. [1495]

Grant, A. P. and L. B. Thomas (1999), "Inflationary expectations and rationality revisited." *Economics Letters*, 62 (3), 331–338. [1493]

Grassi, S. and T. Proietti (2010), "Has the volatility of U.S. inflation changed and how?" *Journal of Time Series Econometrics*, 2 (1), Article 6. [1489, 1508]

Hansen, P. R., A. Lunde, and J. M. Nason (2011), "The model confidence set." *Econometrica*, 79 (2), 453–497. [1486]

Harvey, A. C. (1991), *Forecasting, Structural Time Series Models and the Kalman Filter*. Cambridge University Press, Cambridge. [1493]

Henzel, S. R. (2013), "Fitting survey expectations and uncertainty about trend inflation." *Journal of Macroeconomics*, 35 (1), 172–185. [1487]

Herbst, E. and F. Schorfheide (2014), "Sequential Monte Carlo sampling for DSGE models." *Journal of Applied Econometrics*, 29 (7), 1073–1098. [1505]

Herbst, E. and F. Schorfheide (2016), *Bayesian Inference for DSGE Models*. Princeton University Press, Princeton, NJ. [1496]

Jain, M. (2019), "Perceived inflation persistence." *Journal of Business & Economic Statistics*, 37 (1), 110–120. [1493]

Johansen, A. M. and A. Doucet (2008), "A note on auxiliary particle filters." *Statistics and Probability Letters*, 78 (12), 1498–1504. [1496]

Kass, R. E. and A. E. Raftery (1995), "Bayes factors." *Journal of the American Statistical Association*, 90 (430), 773–795. [1505]

Komunjer, I. and S. Ng (2011), "Dynamic identification of dynamic stochastic general equilibrium models." *Econometrica*, 79 (6), 1995–2032. [1493]

Kozicki, S. and P. A. Tinsley (2012), "Effective use of survey information in estimating the evolution of expected inflation." *Journal of Money, Credit and Banking*, 44 (1), 145–169. [1487, 1493, 1506]

Krane, S. D. (2011), "Professional forecasters' views of permanent and transitory shocks to GDP." *American Economic Journal: Macroeconomics*, 3 (1), 184–211. [1493]

Leeper, E. M. and T. Zha (2003), "Modest policy interventions." *Journal of Monetary Economics*, 50 (8), 1673–1700. [1488, 1512]

Lindsten, F., P. Bunch, S. Särkkä, T. B. Schön, and S. J. Godsill (2016), "Rao–Blackwellized particle smoothers for conditionally linear Gaussian models." *IEEE Journal of Selected Topics in Signal Processing*, 10 (2), 353–365. [1488, 1494, 1498, 1499, 1516]

Liu, J. and M. West (2001), "Combined parameters and state estimation in simulation based filtering." In *Sequential Monte Carlo Methods in Practice* (A. Doucet, N. de Freitas, and N. Gordon, eds.), Chapter 10, 197–223, Springer, Berlin. [1497]

Lopes, H. F. and R. S. Tsay (2011), "Particle filters and Bayesian inference in financial econometrics." *Journal of Forecasting*, 30 (1), 168–209. [1488, 1493, 1497, 1498]

Mackowiak, B. and M. Wiederholt (2009), "Optimal sticky prices under rational inattention." *American Economic Review*, 99 (3), 769–803. [1486, 1513, 1516]

Mankiw, N. G. and R. Reis (2002), "Sticky information versus sticky prices: A proposal to replace the new Keynesian Phillips curve." *Quarterly Journal of Economics*, 117 (4), 1295–1328. [1486, 1490, 1516]

Meltzer, A. H. (2014), *A History of the Federal Reserve: Volume 2, Book II, 1970–1986*. University of Chicago Press, Chicago, IL. [1487, 1503, 1508, 1510]

Mertens, E. (2016), "Measuring the level and uncertainty of trend inflation." *Review of Economics and Statistics*, 98 (5), 950–967. [1487, 1489, 1493, 1512]

Mertens, E., J. M Nason (2020), "Supplement to 'Inflation and professional forecast dynamics: An evaluation of stickiness, persistence, and volatility'." *Quantitative Economics Supplemental Material*, 11, https://doi.org/10.3982/QE980. [1488]

Meyer, L. (1996), "Monetary policy objectives and strategy." Remarks given by Federal Reserve Board Governor Laurence H. Meyer at the *National Association of Business Economists 38th Annual Meeting*, Boston, MA (September 8). [1512]

Morley, J. C., C. R. Nelson, and E. Zivot (2003), "Why are the Beveridge–Nelson and unobserved-components decompositions of GDP so different?" *Review of Economics and Statistics*, 85 (2), 235–243. [1489]

Nason, J. M. and G. W. Smith (forthcoming), "Measuring the slowly evolving trend in US inflation with professional forecasts." *Journal of Applied Econometrics*. [1487, 1488, 1493, 1512]

Nelson, C. R. (2008), "The Beveridge–Nelson decomposition in retrospect and prospect." *Journal of Econometrics*, 146 (2), 202–206. [1489]

Orphanides, A. and D. Wilcox (2002), "The opportunistic approach to disinflation." *International Finance*, 5 (1), 47–71. [1512]

Pitt, M. K., R. dos Santos Silva, P. Giordani, and R. Kohn (2012), "On some properties of Markov chain Monte Carlo simulation methods based on the particle filter." *Journal of Econometrics*, 171 (2), 134–151. [1496, 1497]

Pitt, M. K. and N. Shephard (1999), "Filtering via simulation: Auxiliary particle filters." *Journal of the American Statistical Association*, 94 (446), 590–599. [1496]

Pitt, M. K. and N. Shephard (2001), "Auxiliary variable based particle filters." In *Sequential Monte Carlo Methods in Practice* (A. Doucet, N. de Freitas, and N. Gordon, eds.), Chapter 13, 273–294, Springer, Berlin. [1496]

Särkkä, S. (2013), *Bayesian Filtering and Smoothing*. Cambridge University Press, Cambridge. [1497]

Schorfheide, F., D. Song, and A. Yaron (2018), "Identifying long-run risks: A Bayesian mixed-frequency approach." *Econometrica*, 86 (2), 617–654. [1493]

Shephard, N. (2015), "Martingale unobserved component models." In *Unobserved Components and Time Series Econometrics* (S. J. Koopman and N. Shephard, eds.), 218–249, Oxford University Press, Oxford. [1489]

Sims, C. A. (2003), "Implications of rational inattention." *Journal of Monetary Economics*, 50 (3), 665–690. [1486, 1513, 1516]

Stock, J. H. and M. W. Watson (1999), "Forecasting inflation." *Journal of Monetary Economics*, 44 (2), 293–335. [1486]

Stock, J. H. and M. W. Watson (2007), "Why has US inflation become harder to forecast?" *Journal of Money, Credit and Banking*, 39 (S1), 3–33. [1486, 1487, 1489, 1490, 1500, 1501, 1508, 1512, 1513]

Stock, J. H. and M. W. Watson (2009), "Phillips curve inflation forecasts." In *Understanding Inflation and the Implications for Monetary Policy—A Phillips Curve Retrospective* (J. Fuhrer, Y. K. Kodrzycki, J. S. Little, and G. P. Olivei, eds.), Chapter 3, 99–184, MIT Press, Cambridge, MA. [1486]

Stock, J. H. and M. W. Watson (2016), "Core inflation and trend inflation." *Review of Economics and Statistics*, 98 (4), 770–784. [1487, 1489, 1490, 1508]

Storvik, G. (2002), "Particle filters for state-space models with the presence of unknown static parameters." *IEEE Transactions on Signal Processing*, 50 (2), 281–289. [1497]

Watson, M. W. (1986), "Univariate detrending methods with stochastic trends." *Journal of Monetary Economics*, 18 (1), 49–75. [1489]

Woodford, M. (2003), "Imperfect common knowledge and the effects of monetary policy." In *Knowledge, Information, and Expectations in Modern Macroeconomics: In Honor of Edmund S. Phelps* (P. Aghion, R. Frydman, J. Stiglitz, and M. Woodford, eds.), 25–58, Princeton University Press, Princeton, NJ. [1486]

Co-editor Frank Schorfheide handled this manuscript.

Manuscript received 18 September, 2017; final version accepted 8 May, 2020; available online 2 June, 2020.